

Friedrich-Schiller-Universität Jena
Chemische-Geowissenschaftliche Fakultät
Max-Planck-Institut für chemische Ökologie

Chemical ecology of dinoflagellate-parasite interaction

Masterarbeit

zur Erlangung des akademischen Grades

Master of Science im Studiengang *Chemische Biologie* (M. Sc.)

Vorgelegt von

Yasmin Chaouch

geb. am 21.06.1989 in Dortmund



Jena, 18. Dezember 2019

Erstgutachter

Prof. Dr. Georg Pohnert - Institut für Anorganische und Analytische Chemie, FSU Jena

Zweitgutachter

Dr. rer. nat. Thomas Wichard - Institut für Anorganische und Analytische Chemie, FSU
Jena

Contents

Contents	II
List of Abbreviations	IV
List of figures	V
List of tables	VIII
1. Introduction	1
2. Objective.....	11
3. Material and methods	13
3.1 Materials	13
3.2 Dinoflagellates strains and growth condition	13
3.3 Infection experiments	14
3.4 Metabolic profiling in dinoflagellates-parasite interaction.....	15
3.4.1 Extraction methods and sample preparation	15
3.4.2 UHPLC-HR-MS Parameters	16
3.5 Metabolic profiling in dinoflagellates-copepodamide interaction.....	16
3.5.1 Extraction methods and sample preparation	17
3.5.2 UHPLC-HR-MS Parameters	17
3.6 Data analysis and statistic	17
4. Results & Discussion.....	19
4.1 Growth condition	19
4.1.1 Effects of nutrients supplementation on the growth of dinoflagellate	19
4.1.2 Effects of nutrient supplementation on the growth of infected cells with <i>P. rostrata</i>	21
4.2 Investigations of cellular changes upon parasitic infection	25
4.2.1 Growth rate of infected non-toxic and toxic dinoflagellates.....	25
4.2.2 Metabolic investigation of <i>H. triquetra</i> and <i>A. minutum</i>	27
4.3 Toxin induction assays.....	33
4.3.1 Effect of copepodamides on algal growth performance and infection.....	33
4.3.2 Cell metabolome investigations upon treatment with copepodamide.....	38
4.3.3 Method development for PSP toxin detections	41

Contents

5. Conclusion	46
References	48
Appendix	i
Appendix for Chapter 4.2	i
Appendix for Chapter 4.3	iv
Zusammenfassung	x

List of Abbreviations

ANOVA	Analysis of Variance
A. spp.	<i>Alexandrium</i> spp.
AM	<i>Alexandrium minutum</i>
DNA	Deoxyribonucleic acid
ESI	Electrospray Ionization
EtOH	Ethanol
GTX	Gonyautoxin
H. spp.	<i>Heterocapsa</i> spp.
HAB	Harmful algal blooms
HT	<i>Heterocapsa triquetra</i>
MeOH	Methanol
MS	mass spectrometry
P. spp.	<i>Parvilucifera</i> spp.
PCA	Principal component analysis
PLS-DA	Partial least squares-discriminant analysis
PSP	Paralytic shellfish poisoning
QC	Quality Control
RT	Retention time
spp.	Species pluralis
STX	Saxitoxin
UHPLC-HR-MS/MS	Ultra-High Performance Liquid Chromatography High-Resolution Mass Spectrometry

List of figures

Figure 1 Algal bloom and its economic impact. Adapted from Sanseverino <i>et al.</i> (2016) ³⁰	2
Figure 2 Theoretical transmembrane structure of the voltage-dependent sodium channel. Adapted from https://www.spektrum.de/lexikon/biologie/natriumkanale/45413 (01.12.2019) ⁵¹	4
Figure 3 Structure and species of Saxitoxins-Derivates from marine dinoflagellates (Figure from Wang, D. Z. <i>et al.</i>) ⁵⁴	5
Figure 4 Part of biotransformations of PSP. Adapted from Wiese <i>et al.</i> (2010) ¹⁹	6
Figure 5 General life cycle of aquatic zoosporic parasites of phytoplankton (permission to reuse, License Number 4730720039248) ⁸⁴	8
Figure 6 a) Growth curves of healthy <i>A. minutum</i> grown in three different culture media (F/2 with silicate supplementation, F/2 –Si no silicate supplementation, Penzé medium) either as untreated (healthy cultures). b) Cell density and c) growth rates of <i>A. minutum</i> grown in three different culture media (F/2 with silicate supplementation, F/2 –Si no silicate supplementation, Penzé medium). The average values of the growth rates are shown along with the standard deviation. A Student’s test found statistical significance between the F/2-mediums and Penzé medium (* for P-value < 0.05).	20
Figure 7 a) <i>A. minutum</i> treated with cells infected by <i>Parvilucifera rostrata</i> . The average values of the cell densities are shown along with the standard deviation. N = 3 for both experiments. b) Cell density and c) growth rates of <i>A. minutum</i> grown in three different culture media (F/2 with silicate supplementation, F/2 –Si no silicate supplementation, Penzé medium) for cells infected by <i>Parvilucifera rostrata</i> . (one way ANOVA, * for P-value < 0.05).....	22
Figure 8 a) Infection rate of <i>P. rostrata</i> infecting <i>Al. minutum</i> evaluated in three different culture media (F/2 with silicate supplementation, F/2 –Si no silicate supplementation, Penzé medium) Cell counts of parasitic trophocysts (b) and sporangia (c) in infected <i>A. minutum</i> cultures in three different culture media (F/2 with silicate supplementation, F/2 –Si no silicate supplementation, Penzé medium). Representative microscopy pictures from Alacid <i>et al.</i> Scale bars equal 20 µm. ⁸⁵	23
Figure 9 Culture of treated and untreated <i>H. triquetra</i> after 16 days of incubation	25

List of figures

Figure 10 Growth rate of <i>H. triquetra</i> grown in Penzé medium and treated with <i>P. rostrata</i> (RCC2852) and <i>P. infectans</i> (RCC2824).....	26
Figure 11 Growth rate of <i>A. minutum</i> grown in Penzé medium and treated with <i>P. rostrata</i> (RCC2852) and <i>P. infectans</i> (RCC2824).....	27
Figure 12 Metabolic investigation of dinoflagellate <i>H. triquetra</i> during infection by parasites <i>Parvilucifera</i> spp. a) Total ions chromatograms depicting the pool samples analyzed four times thorough the UHPLC-MS/MS run in positive and negative polarities. b) Significant changes in the metabolic content of <i>H. triquetra</i> cells healthy or infected either by <i>P. rostrata</i> or <i>P. infectans</i>	29
Figure 13 Significant changes in metabolic content of healthy or infected cells of <i>A. minutum</i> found by PLS-DA analysis.....	30
Figure 14 Chemical structure of the synthetic analog (unpublished results, Ph.D. Marino Wirgenings). ⁹¹	33
Figure 15 Cell densities of <i>A. minutum</i> RCC3008 treated with 1 nM of extracts mixture of copepodamides, synthetic copepodamide or methanol. The average values are shown along with the standard deviation. A Student's test found statistical significance between control and treatment (* for P-value < 0.01), but not for all independent experiments....	35
Figure 16 Cell densities of <i>A. minutum</i> (RCC2663, RCC1490, RCC2672, RCC3008) and <i>H. triquetra</i> (HT) grown for 2 days with synthetic copepodamide or with methanol (0.1%). The average values are shown along with the standard deviation. A Student's test found statistical significances for <i>Alexandrium</i> cells treated with copepodamide and those with methanol (N = 4, for RCC2663 t = -6.140 P-value < 0.001, for RCC1490 t = -2.828 P-value = 0.03, for RCC2672 t = -4.700 P-value = 0.003, for RCC3008 t = -5.555 P-value = 0.001).	36
Figure 17 Growth rates of <i>A. minutum</i> (RCC2663, RCC1490, RCC2672, RCC3008) and <i>H. triquetra</i> (HT) grown for 6 days in Penzé medium and were infected with <i>P. rostrata</i> 3 days after treatment with copepodamies. The average values are shown along with the standard deviation. A Student's test did not found statistical significance between copepodamide and methanol treatment (N = 4, P-value = 0,201).	37
Figure 18 Significant changes in metabolic content of untreated or treated cells of <i>A. minutum</i> found by PCA analysis.....	39

List of figures

- Figure 19** PSP toxins detection with UHPLC-HR-MS/MS in cell extracts of *A. minutum* RCC3008. The 300.1409, 257.1352 and 316.1359 m/z for $[M+H]^+$ assigned to decarbamoyl saxitoxin, Saxitoxin (SXT), neosaxitoxin (neoSXT) are detected at 0.8 min, respectively. 43
- Figure 20** A) Extract ion chromatogram of *Alexandrium* cell extracts (sample E8_C19_AM176 for strain RCC3008) analyzed by UHPLC-HR-MS in positive polarity and mass spectrum with the detected m/z in bold for saxitoxin ($C_{10}H_{17}N_7O_4$ expected 300.1414 m/z for $[M+H]^+$) B) Extract ion chromatogram of *Alexandrium* cell extracts (sample E8_C19_AM176 for strain RCC3008) analyzed by UHPLC-HR-MS in positive polarity and mass spectrum with the detected m/z in bold for decarbamoylsaxitoxin ($C_9H_{16}N_6O_3$ expected 257.1356 m/z for $[M+H]^+$)..... 44
- Figure 21** Extract ion chromatogram of *Alexandrium* cell extracts (sample E8_C19_AM176 for strain RCC3008) analyzed by UHPLC-HR-MS in positive polarity and mass spectrum with the detected m/z in bold for gonyautoxin 2 ($C_{10}H_{17}N_7O_8S$ expected 396.0932 m/z for $[M+H]^+$)..... 45

List of tables

Table 1 Parasites and dinoflagellates strains employed in this study	13
Table 2 Composition of the F/2 Guillard's nutrients solution (G9903, G0154 without silicate, Sigma-Aldrich). 20 ml of this solution was added to 1L of marine seawater (PSU35)....	14
Table 3 Selected metabolites from one-way ANOVA test with a proposed identity (class), retention time (RT), observed ion traces and identity score (CSI %) found by MS/MS spectral similarity search with the public database. In bold is one of the most significant metabolites discriminating infected from healthy extracts of <i>A. minutum</i> . (Up-regulated in: *all treated cells; **RCC2857; ***healthy cells).....	31
Table 4 Metadata of the toxin induction experiments with synthetic copepodamides	34
Table 5 Metadata of the toxin induction experiments with natural extracts copepodamides..	34
Table 6 Selected metabolites from one-way t-test with a proposed identity (class), retention time (RT), observed ion traces and identity score (CSI %) found by MS/MS spectral similarity search with the public database (They are all up regulated in treated cells).....	40
Table 7 Selected metabolites from one-way t-test with a proposed identity (class), retention time (RT), observed ion traces and identity score (CSI %) found by MS/MS spectral similarity search with the public database.....	41

1. Introduction

Protistan phytoplankton has a major role in the ecosystem of our planet. They are various primarily unicellular organisms that occur both in oceans and in freshwater. Although their photosynthetic biomass makes up only 1% of the earth, they are responsible for about 50% of the earth's total photosynthesis.^{1, 2} They are also involved in CO₂ respiration by converting CO₂ into organic carbon through photosynthesis, which makes them a key role in biogeochemical processes.³ Unfortunately, due to rising sea temperatures, the amount of marine phytoplankton has been decreasing sharply since 1950.⁴ Phytoplankton includes a large variety of cyanobacteria, algae and microalgae such as dinoflagellates.⁵

These are microalgae that form a significant part of the primary planktonic production in water bodies.⁶ Two flagella are characteristic of their structure, providing them with the propulsive force to move in the water and maintain it in the water column based on the availability of nutrients. Although it is usually due to asexual cleavage that dinoflagellates reproduce, sexual reproduction also occurs in some species that determine the formation of dormant cells called cysts.⁷ The dinoflagellates can be classified into two major lineages, the syndineans and the core dinoflagellates.^{8, 9} The core dinoflagellates are formally called dinokaryotes in which the nucleus stays a dinokaryon (eukaryotic nucleus) for the entire cell cycle.¹⁰ Syndineans include a group of intracellular parasitic dinoflagellates. They can be distinguished from the main group by the absence of dinocaryotes or the absence of the typical cell wall.⁹ Another special feature of dinoflagellates is that they have a high diversity of alternative nutritional modes. They can be phototrophic, heterotrophic or mixotrophic. Furthermore, they may be either symbiotic or parasitic.¹¹⁻¹⁵ *Amoebophrya* sp is a parasitic dinoflagellate.¹⁴ Moreover, they can interact intra- as well as interspecifically via semiochemicals, which influences, for example, the bloom dynamics.¹⁶ Dinoflagellates, such as *Alexandrium* spp., *Gymnodinium* spp. and *Pyrodinium* spp., are mainly responsible for harmful algal blooms (HABs) that occur worldwide.¹⁷⁻²⁵ They are globally widespread, but without appearing in polar or subpolar regions.²⁶ These HABs have a significant impact on the ecosystem of the ocean.²⁷ During these HABs, there is a possibility that fish may absorb the toxins, which can lead to disruption of the fish trade and consequently to a significant

1. Introduction

economic loss. This leads, among other things, to an increase in the cost of food from the sea, in addition to fish, other living organisms such as oysters are also affected.²⁸ The United Kingdom, for example, has a loss of 29,000 to 180,000 £ per year due to HABs in freshwater.²⁹

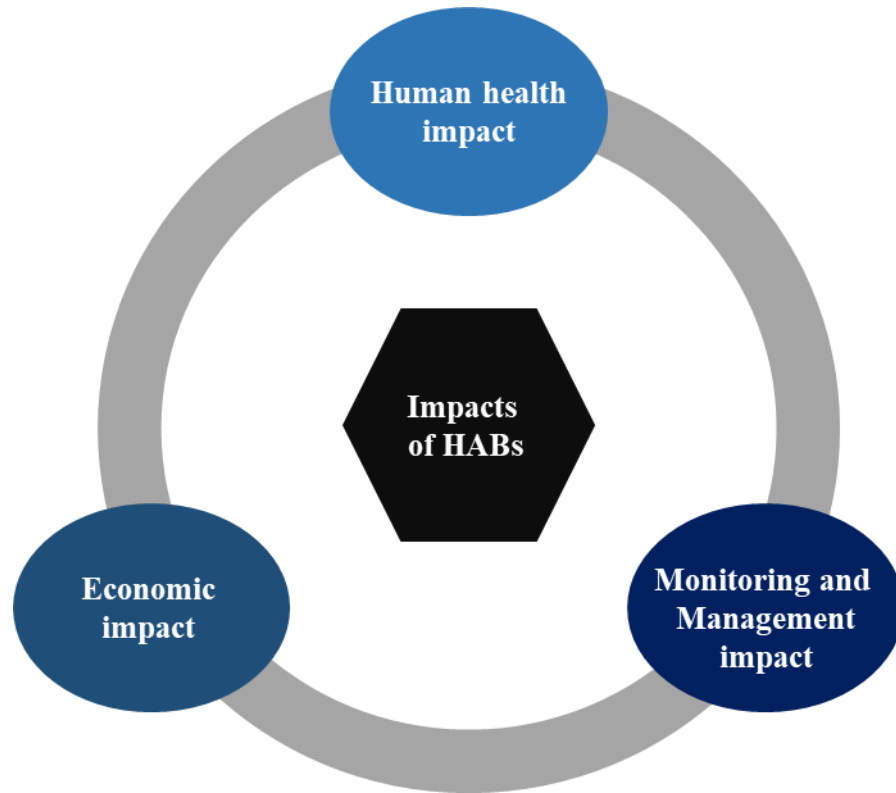


Figure 1 Algal bloom and its economic impact. Adapted from Sanseverino *et al.* (2016)³⁰

In addition to the economic factor, there is also a great impact on human health.^{28, 31, 32} Human exposure to toxins can occur in various ways, such as contamination by direct contact with water through swimming, as well as ingestion through drinking water or consuming contaminated food.^{33, 34} The number of these toxic blooms and the resulting consequences have increased dramatically. A not insignificant part of this expansion is due to humans, for example by added massive and increasing amounts of industrial and agricultural wastewater into coastal waters. This leads to an increased growth rate of the algae population.³⁵ In consequence of this, monitoring, as well as control and management of the HABs, becomes indispensable.³⁵⁻³⁷ A class of this possible toxins is the paralytic shellfish poisoning (PSP)

1. Introduction

which are produced by dinoflagellates of the genera *Alexandrium*, *Gymnodinium* and *Pyrodinium*.¹⁷⁻²¹

The dinoflagellate genus *Alexandrium* belongs to the potentially most toxic phytoplankton species, of which 28 species are documented, including 11 classified as toxic. The life cycle of dinoflagellates comprises multiple stages with different morphology, physiology, function and often seems to complement each other from different mechanisms in the same species.³⁸ According to the general scheme, it is a zygotic life cycle that begins with the vegetative phase. In asexual reproduction, the cell divides by desmoschisis, some *Alexandrium* spp. transform into cysts that perform cell division. During the sexual phase, the vegetative cells form gametes. These gametes can recognize each other with the help of agglutinin-like compounds, conjugate with each other and form diploid planozygotes. These, in turn, can undergo meiosis in some species. At the resting state, this zygote becomes a hypnozygote. At cold temperatures or external stress factors, the maturation period of the hypnozygote can be prolonged. Especially in the case of temperature differences, it can, therefore, be called a seasonal flowering period. During germination of hypnozygotes, a planomeiocyte is formed and the sexual cycle is completed.^{39,40}

Besides the variation of asexual and sexual reproduction, *Alexandrium* also has a variation in the toxin profile.^{24, 41} In addition to *Alexandrium minutum*, the production of PSP toxins for *A. funyense*, *A. andersonii*, *A. catenella*, *A. tamarense*, and *A. pacifium* could also be confirmed.⁴²⁻⁴⁶ This neurotoxic alkaloid is chiefly saxitoxin (STX) and its derivatives. According to the literature, 57 analogs of STX are known. The consequence of these toxins is the already mentioned HABs, which pose a great danger, especially for humans.¹⁹

The human has the highest sensitivity, at a lethal oral dose of about 1-4 mg (Saxitoxin), against the toxin.⁴⁷ Toxins selectively block the voltage-controlled sodium channel of excitable membranes which inhibits the production and spread of action potentials in nerve axons and skeletal muscle fibers.⁴⁸ This happens through the interaction of the positively charged guanidinium groups of STX with the negatively charged carboxyl groups of the Na⁺ channel at the IV domain of the alpha subunit.^{49, 50}

1. Introduction

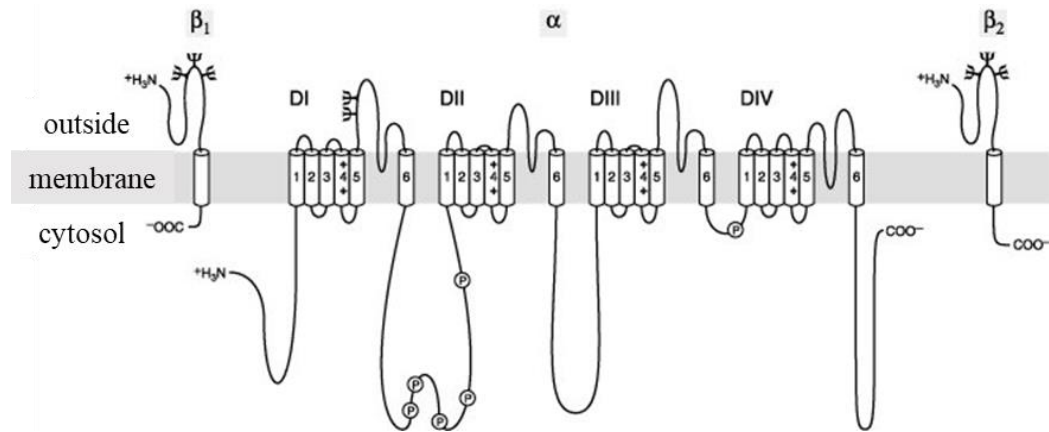
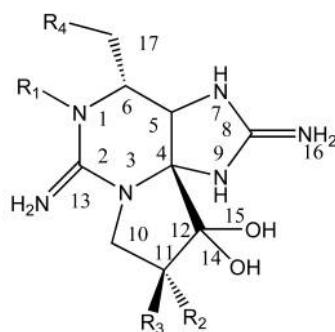


Figure 2 Theoretical transmembrane structure of the voltage-dependent sodium channel. Adapted from <https://www.spektrum.de/lexikon/biologie/natriumkanale/45413> (01.12.2019)⁵¹

These PSPs can be hydrophilic or hydrophobic. SXT is one of the strongest natural neurotoxins known.⁵² In 1957 STX was the first PST isolated in pure form from the Alaskan butter clam, *Saxidomus gigangteus*.⁵³ The alkaloid SXT has the molecular formula $C_{10}H_{17}N_7O_4$ and is composed of a tricyclic 3,4-propinoperhydropurine tricyclic ring and a carbamate. Due to the two guanidine groups, the molecule has a high polarity and is therefore water-soluble. A few possible derivatives are shown in Figure 3. Dinoflagellates, like other organisms, often produce a mixture of STX and STX derivatives.⁵⁴⁻⁵⁹ For *A. minutum*, for example, a mixture of SXT, GTX2 and GTX3 could be detected in Irish coastal waters.²⁵

1. Introduction



	Toxin	R1	R2	R3	R4
Carbamate	STX	H	H	H	OCONH ₂
	Neo STX	OH	H	H	OCONH ₂
	GTX1	OH	OSO ₃ ⁻	H	OCONH ₂
	GTX2	H	OSO ₃ ⁻	H	OCONH ₂
	GTX3	H	H	OSO ₃ ⁻	OCONH ₂
	GTX4	OH	H	OSO ₃ ⁻	OCONH ₂
	N-sulfocarbamoyl	GTX5(B1)	H	H	H
GTX6(B2)		OH	H	H	OCONHSO ₃ ⁻
C1		H	OSO ₃ ⁻	H	OCONHSO ₃ ⁻
C2		H	H	OSO ₃ ⁻	OCONHSO ₃ ⁻
C3		OH	OSO ₃ ⁻	H	OCONHSO ₃ ⁻
	C4	OH	H	OSO ₃ ⁻	OCONHSO ₃ ⁻
Decarbamoyl	dcSTX	H	H	H	OH
	dcNeoSTX	OH	H	H	OH
	dcGTX1	OH	OSO ₃ ⁻	H	OH
	dcGTX2	H	OSO ₃ ⁻	H	OH
	dcGTX3	H	H	OSO ₃ ⁻	OH
	dcGTX4	OH	H	OSO ₃ ⁻	OH
Deoxydecarbamoyl	doSTX	H	H	H	H
	doGTX2	H	H	OSO ₃ ⁻	H
	doGTX3	H	OSO ₃ ⁻	H	H

Figure 3 Structure and species of Saxitoxins-Derivates from marine dinoflagellates (Figure from Wang, D. Z. *et al.*)⁵⁴

The analog differs in the selection of the substituents of the side chains, the most known toxins so far are hydrophilic.⁵² The different levels of toxicity are depending on the substituent of the side chains. The substitution on R₄ has defined the group of the respective toxin, which includes carbamate toxins (STX, neo-STX, GTX1-4), N-sulfocarbamoyl toxins (GTX5-6, C1-4), decarbamoyl toxins (dcSTX, dcNeo-STX, dcGTX1-4) and deoxydecarbamoyl toxins (doSTX, doGTX2-3).^{54, 60-63} The only more toxic STXs derivative than STX itself is zetekitoxin AB, which isolated from the gold frog *Atelopus zeteki*.

1. Introduction

The structure of zetekitoxin has a unique 1,2-oxazolidine ring fused lactam.^{19,64} The biosynthetic pathway for STXs in STX-producing organisms is little known. The only available information on the biosynthesis of STXs proved that the skeleton of STXs is synthesized from arginine and acetate.⁶⁵

Biotransformation can lead to changes in the PSP toxin profile and thus to new toxins that cannot be biosynthesized by cyanobacteria or dinoflagellates alone.^{19, 63}

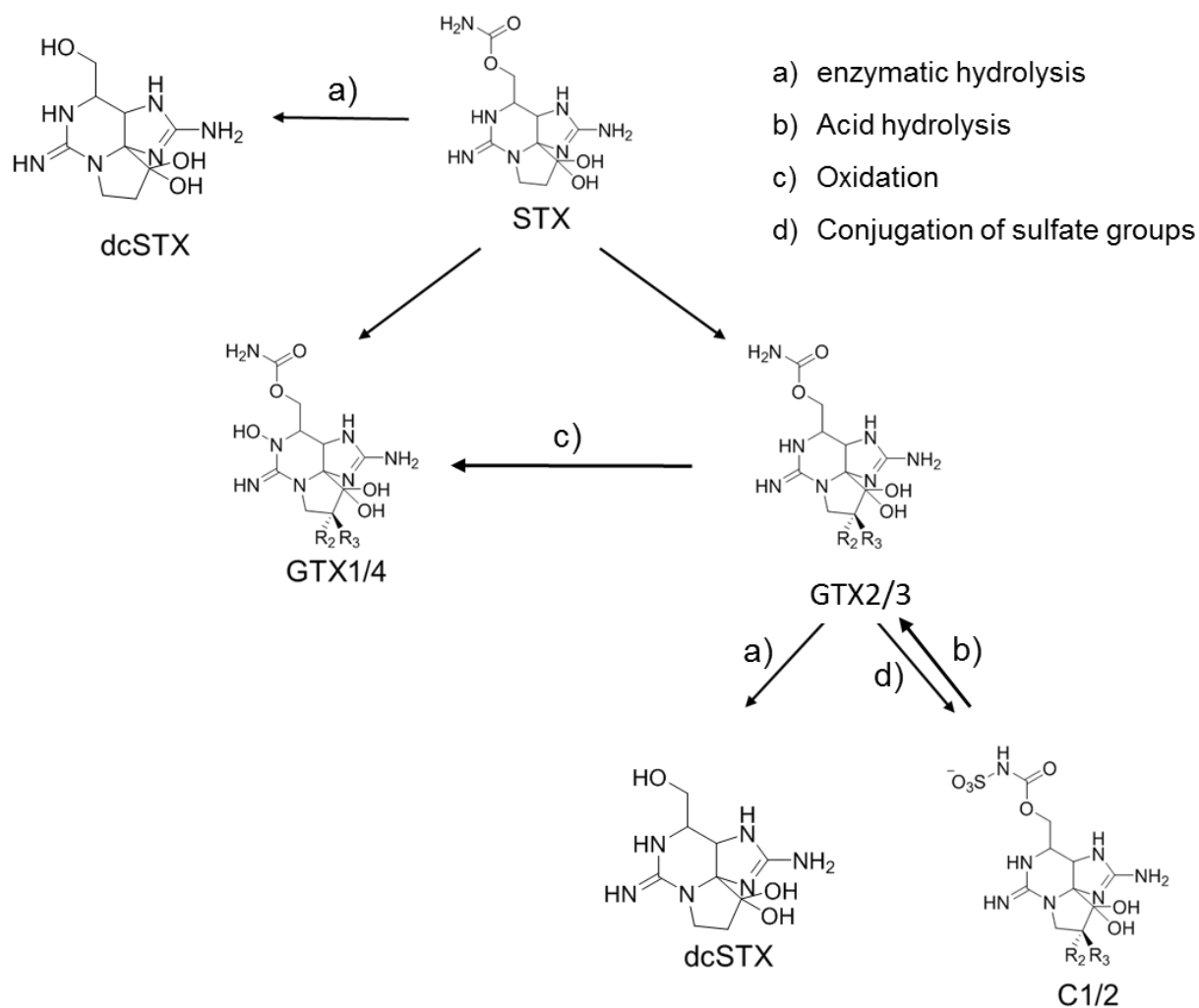


Figure 4 Part of biotransformations of PSP. Adapted from Wiese *et al.* (2010)¹⁹

In the biotransformation of STX, both functionalization reactions (reduction, hydrolysis, oxidation) and conjugation reactions (conjugation of glucuronic acid, conjugation of a sulfate part) were observed.¹⁹

1. Introduction

There is a probability that inherent STX enzymes are involved in biotransformation in some organisms.⁶⁶ The enzymatic hydrolysis of the carbamat group and N-sulfocarbomoyl toxins into the decarbamoyl toxins could be observed in the small neck clam *Prothotheca stamnea*.⁶⁷ The acid hydrolysis of the relatively non-toxic N-sulfocarbomoyl toxins C1/2 in GTX2/3, which exhibit high toxicity, within a homogenate of the scallop *Placopecten magellanicus* could also be observed.^{67, 68}

Furthermore, biotransformations were also found within dinoflagellates. During the incubation of *A. taarense* homogenate with GTX2/3, it was oxidized to GTX1/4.⁶⁹ During the incubation of carbamoyl toxins with *G. catenatum* homogenate a conjugation of sulfate groups and therewith a conversion to C1/2 toxins could be observed.⁷⁰

In this context, it is also important to study predators and parasites of dinoflagellates and their reaction as well as their influence on the metabolism of dinoflagellate, include the toxin production. Some algae, for example, modulate their toxin production in response to chemical evidence from predators.⁷¹ The most successful form of nutrition is parasitism and the presence of parasitic organisms is abundant in most ecosystems. This is also the case for marine planktonic ecosystems, where a wide variety of parasitic species is known.⁷² Prokaryotic, as well as eukaryotic organisms, can be parasitoids of dinoflagellates; viruses and bacteria occur less frequently in them.⁷³ In most cases, they are infected by eukaryotic parasitoids.^{72, 74}

A lot of data is known about the parasitoid of the family *Parviluciferaceae*.⁷⁵ The Phylum of *Parviluciferaceae* is Perkinsozoa. Perinsozoa occurs in various waters, including marine waters.⁷⁶ In the beginning, it was only assumed that they formed a sister group of dinoflagellates.⁷⁷ For the first time, they could be classified in 1950 in the fungus *Perkinsus marinus*.⁷⁸ In 1997 further analysis of the DNA sequences was carried out, which came to the conclusion that Perinsozoa is indeed related to the dinoflagellates.⁷⁹

Parvilucifera parasitoid is a genus of marine alveolates from *Parviluciferaceae* that infected dinoflagellates. Especially for *P. infectans*, *P. sinerae* and *P. rostrata*, solid literature is available as a basis for further research.^{17, 75, 80-83}

1. Introduction

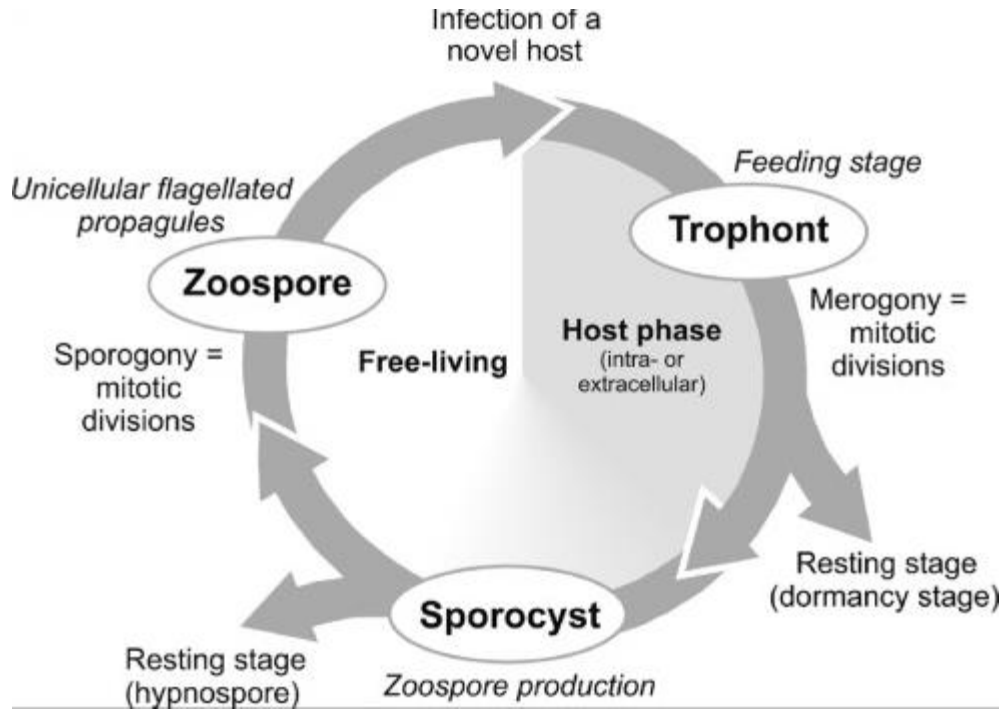


Figure 5 General life cycle of aquatic zoosporic parasites of phytoplankton (permission to reuse, License Number 4730720039248)⁸⁴

The general life cycle of a parasite like *Parviluciferaceae* goes through 3 phases. First, the host is infected by contact with wild zoospores.⁸⁴ At this stage of infection, a dinoflagellate is the first to lose its flagella and the associated motility.⁸¹ The infection initiated by this leads to the parasite becoming a trophocyte. The parasite enters the food phase and its host is partially or completely utilized. The host can have more than one trophocyte. It is also possible for trophocytes to undergo mitotic cell division. Depending on the host and parasite, the trophocyte changes into sporangia. This last stage describes the transition to the release of the newly formed zoospores.⁸⁴ By microscopy, an infection of dinoflagellates, as in *A. minutum*, with parasitoids can be well quantified.^{17, 81}

P. infectans, *P. sinerae*, *P. rostrata* and other parasites of this genus are mostly generalists who infected a wide range of dinoflagellates. But there are also some parasites there are specifist from *Parvilucifera* who prefer a genus of dinoflagellates such as *Alexandrium*.⁸⁵⁻⁸⁷ Furthermore, all of them kill their host by reaching their life cycle, which is why they are called parasitoids.⁸⁴ The use of these parasitoids is proposed by some researchers as a

1. Introduction

biological control against HABs.^{88, 89} However, the unintended side effects on other dinoflagellates are still unknown.³⁵

In addition to parasitoids, dinoflagellates also have natural predators such as copepods. Copepods belong to a small Crustacean group. Due to the high number they belong to one of the most common metazoic groups. They are well suited as model organisms in ecological and evolutionary studies. Copepodamides originally come from marine waters, but they are also often found in many freshwaters.⁹⁰ They have an exoskeleton, conspicuous first antennae, and a single, simple anterior eye. Their swimming legs, each pair of which are connected at the base by a "coupling" or an "intercoxal sclerite".⁹⁰

The survival strategies of the dinoflagellates include changes in colony size, swimming behavior and the indication of toxin formation. *A. minutum*, for example, experience a drastic increase in toxicity when exposed to direct contact with copepods or chemical signals triggered by copepodamides.⁹¹ *A. minutum* can recognize waterborne signals of the predator and react to them. Also, increased resistance of the dinoflagellate to recurrent contact with copepodamides could be observed. The increased resistance also leads to an increased growth rate of the resistant dinoflagellates.⁹² This could lead in the future to grazers changing their prey behavior and prefer non-toxic dinoflagellates instead of toxic dinoflagellates.⁹³ Nevertheless, increased toxin production could also have a benefit by reducing pasture pressure on identical cells.⁹⁴ If grazers were physically incapacitated by the ingestion of toxic cells, however, they would also benefit from less toxic or non-toxic prey.⁹²

The detection of toxins requires appropriate analytical methods to clearly detect and quantify them. Non-chromatographic methods, such as the use of a bioassay, still form the basis for a large number of monitoring procedures today.⁹⁵ The mouse bioassay provides clear information on the toxic potential of a sample, but it is not possible to specify the toxins. Furthermore, the mouse bioassay is not suitable for studies on the formation and effect of individual PSP toxins.⁹⁶

One of the first steps in the chromatographic determination of toxins in the development of an alkaline oxidation process for STX. Under alkaline conditions in combination with oxidation, the ring breaks between C12 and C14.^{97, 98} During a subsequent treatment with an acidic

1. Introduction

milieu, the corresponding lactam, a pyrimidinopurine, is formed. This new ring closure results in an increased fluorescence at 210, 260 and 325 nm which can be detected chromatographically.⁹⁹ However, the methods based on the oxidation and fluorescence test do not allow the discrimination of individual toxins, so it is essential to know which PSP components are present in the sample.¹⁰⁰ For the unambiguous identification, more accurate methods of analysis are suitable, HPLC is the most common method. It has the necessary sensitivity to distinguish the individual analogs and also enables their separation. For this purpose, both the method of ion pair chromatography and that of ion exchange chromatography can be applied.^{101, 102}

The already known fluorescence method is suitable for the detection of the separated toxins. The oxidation of the STX, which is necessary for this detection, can be performed pre-column as well as post-column.^{103, 104} Mass spectrometric detection is another established method. The mass spectrometer detects the mass to charge ratio of each component and thus enables a good differentiation of the individual STX analogs.¹⁰⁵

The use of ion-pairing reagents to ensure sufficient retention of STXs has the disadvantage of decrease the sensitivity of MS detection. This circumstance can be circumvented by the separation of ion-exchange chromatography.¹⁰¹ Fragmentation yields high-resolution mass spectra that allow identification of the compounds based on the specific metabolic fingerprint, which can be matched with the mass spectra of a database such as SIRIUS-CSI:FingerID. For an accurate determination of the STX and other metabolites, however, an independent detection of the mass spectrum of the supposed structure is necessary for further comparison.

2. Objective

2. Objective

Harmful algal blooms (HABs) can be formed by toxic dinoflagellates species that produced diverse small molecules and can threaten human activities and coastal life. The paralytic shellfish poisoning (PSP) is a disease resulting from the consumption of algal toxins that accumulate along the food chain and in seafood such as oysters, mussels, clams. Strikingly, copepodamides produced by the predators of the dinoflagellates, the copepods grazers, can elicit the production of these toxins and hence represent a useful tool for establishing and investigating algal toxicity in the lab. During these harmful blooms, many other microorganisms are recruited and especially flagellated parasites such as eukaryotes *Parvilucifera* that can infect and decimate entire populations of toxic dinoflagellates.¹⁰⁶ These generalist parasites from the phylum Perkinsozoa are able to infect many different dinoflagellate species and can thrive under different environmental conditions, using different resources. However, why some dinoflagellates species are more susceptible to parasitic infections have not yet been answered.

In this context, we want to investigate if cellular metabolic changes in toxic dinoflagellates in various conditions might be responsible for different susceptibility to parasites and if toxic algae are more infected by *Parvilucifera* than non-toxic ones. Three main experimental setups were employed to investigate the model *Parvilucifera*-dinoflagellates. Using infection experiments, the effect of the nutrients medium was assessed on the growth of *Alexandrium minutum* healthy and parasite-treated cells. On another hand, the cell metabolomes of very susceptible *A. minutum* and low susceptible *Heterocapsa triquetra* were investigated with UHPLC-HR-MS and comparative metabolomics. We hypothesized that some metabolic predictors could predict the disease and want to investigate the metabolic differences between very and low susceptible host cells. Finally, we hypothesized that *Parvilucifera* spp. might prefer toxic host to non-toxic ones and we applied a series of experiments involving a copepodamides extract and a synthetic analog to establish toxic strains. We used UHPLC-MS to detect algal Saxitoxin and related derivatives.

2. Objective

The three main points that have been focused on here are as follows:

1. Infection experiment

A series of experiments with *A. minutum* and *Parvilucifera*. What effect does the selection of the medium have on the growth of healthy cells? How does the infection change depending on the choice of medium? Is there a difference in the susceptibility of different dinoflagellates to different parasitoids?

2. Investigations of cell metabolomes changes upon infection

For the detection of cellular metabolic changes in toxic dinoflagellates an analytical method using UHPLC-MS/MS will be developed. It will be investigated whether different *Parvilucifera* species indicate the same metabolic change in the same host and how they differentiate in two hosts. Can some metabolic predictors predict the disease? Are there more resistant strains?

3. Investigation of the infection resistance through toxin production

It is believed that the microalgae induced by the toxin production via copepodamide production have an increased resistance to the parasitoid. For this purpose, a natural extract of copepodamide and for the first time, an analogous synthetic product was used. The development of a method for the detection of the saxitoxin family and the investigation of the effect of the copepodamides was another important step. How do both copepodamides influence the growth of different dinoflagellates? After treatment with copepodamides, did dinoflagellates show higher resistance to parasitoids?

3. Material and methods

3.1 Materials

All chemicals and solvents have been purchased from Sigma-Aldrich and used without further treatment unless otherwise stated.

To investigate the effects of bioactive lipids from the predators of dinoflagellates, the copepodamide extracts, and a synthetic analog was provided by Erik Selander (University of Gothenburg, Sweden) and Marino Wirgenings (Ph.D. doctorate, Pohnert group, Friedrich Schiller University), respectively.

3.2 Dinoflagellates strains and growth condition

The dinoflagellates and parasites strains were isolated in France (Penzé Estuary) and provided from the Roscoff Culture Collection (Table 1). The dinoflagellates *A. minutum* and *H. triquetra* were grown in the F/2 culture medium, F/2 medium without Si and Penzé medium. The concentrations of the nutrient components of the medium are shown in Table 2. Unless described otherwise, the cultivation was carried out during a 14-hour photoperiod illuminated at a $100 \mu\text{mol}\cdot\text{m}^{-2}\cdot\text{s}^{-1}$ irradiance coupled with a thermoregulation cycle (19 °C / 17 °C day/night).

Table 1 Parasites and dinoflagellates strains employed in this study

Host/parasite	Species name	Strain code
Host	<i>Alexandrium minutum</i>	RCC3008 (AM176)
Host	<i>Alexandrium minutum</i>	RCC1490
Host	<i>Alexandrium minutum</i>	RCC2663
Host	<i>Alexandrium minutum</i>	RCC2672
Host	<i>Heterocapsa triquetra</i>	HT150
Parasite	<i>Parvilucifera rostrata</i>	RCC2857
Parasite	<i>Parvilucifera infectans</i>	RCC2824

3. Material and methods

Table 2 Composition of the F/2 Guillard's nutrients solution (G9903, G0154 without silicate, Sigma-Aldrich). 20 ml of this solution was added to 1L of marine seawater (PSU35).

Component	Concentration (mg L ⁻¹)
Biotin	0.005
CoCl ₂ •6H ₂ O	0.010
CuSO₄•5H₂O	0.010
EDTA disodium • 2H ₂ O	4.360
FeCl ₃ 6H ₂ O	3.150
MnCl ₂ • 4H ₂ O	0.180
Sodium metasilicate • 9H ₂ O	15.000
Na ₂ MoO ₄ • 2H ₂ O	0.006
NaNO ₃ • 2H ₂ O	75.000
BaH ₂ PO ₄	4.411
Thiamine • HCl	0.100
Vitamin B ₁₂	0.005
ZnSO ₄ • 7H ₂ O	0.022

3.3 Infection experiments

To assess the effect of medium on *Parvilucifera rostrata* infection, 14 days old cells of the dinoflagellate *A. minutum* were added to 40 ml of medium, adjusting the initial cell density to 90 000 cells·ml⁻¹. The cultures were carried out in cell flask (Sarsted AC & Co, Germany). 250 µl of *Parvilucifera rostrata* sporangia were inoculated and the cultures were incubated for 20 days.

Controls consisted of uninfected dinoflagellates cultures. To determine the cell density, the cultures were homogenized, fixated with Lugol 0.1% and 10 µl were added to a Neubauer chamber (dimension 0.100 mm). The formula used was:

$$\frac{\text{cell}}{\mu\text{L}} = \frac{\text{number of cells}}{\text{numbers of squares}} \times 10.000$$

The growth rate was calculated using the following formula:

$$\text{growth rate} = \frac{\ln\left(\frac{N_t}{N_0}\right)}{\Delta t}$$

3. Material and methods

N_t and N_0 represent the cell densities at time t and time 0. The time difference between the measurements is described as Δt in days.¹⁰⁷

To determine the prevalence of the infection, the number of sporangia was counted in the Sedgwick Rafter chamber (Pyser-SGI, Kent, UK) cell following Garces *et al.*¹⁰⁸ without the addition of Lugol. The infection rate is calculated from the following formula:

$$\text{Infection rate in \%} = \frac{\text{Total cell number} - \text{infected cells}}{\text{Total cell number}} \times 100$$

The software SigmaPlot version 14.0 was used for the statistical comparison of the cell densities, growth rates and infection prevalence.

The cells were observed with an Olympus inverted microscope and pictures were taken with a camera connected to a stereomicroscope (binocular visiScope®, VWR International GmbH, Pennsylvania, US). All experiments were performed in triplicates unless stated otherwise.

3.4 Metabolic profiling in dinoflagellates-parasite interaction

To investigate the cellular metabolome changes during *Parvilucifera* infection, the analysis of cellular and exudate extracts was performed with ultra-high performance liquid chromatography coupled to high-resolution mass spectrometry (UHPLC-HR-MS). We analyzed two different algal species, *A. minutum* and *H. triquetra*, which were cultivated with parasites *P. rostrata* or *P. infectans*.

3.4.1 Extraction methods and sample preparation

The cell cultures were extracted in filter tunnel heads (glass beakers, PP funnels, seals from DURAN, Mainz, Germany) with filter discs with glass edges (DURAN, Mainz, Germany), GF/C filters (24mmØ, pore size 4, glass edge, VWR International GmbH, USA) and a vacuum pump.

The filter cake was then placed together with the filter of each sample in a 2 ml Eppendorf tube. Afterward, 1.8 mL of the respective solvent were added, a solution of MeOH:EtOH:CHCl₃ 1:3:1 for *H. triquetra* and a solvent of pure MeOH for *A. minutum*

3. Material and methods

were used. The total volume of each tube was transferred to new tubes. The new tubes, without filters, were centrifuged for 15 min and 13000 rpm. Thereafter, the supernatant was added in glass vials with appropriate screw caps (MACHEREY-NAGEL GmbH & Co. KG, Düren, Germany) and dried in a concentrator (Concentrator plus/Vacufuge® plus, Eppendorf, Germany). The dried stock solution was stored at -20°C in the freezer. In order to normalize the cell concentration, the volumes used were normalized using the volume for sample E16. The quantities used for the stock solutions are shown in the following table 3, chapter 4.2.

The supernatants were transferred into corresponding screw caps (MACHEREY-NAGEL GmbH & Co. KG, Dueren, Germany) and dried with a concentrator (Concentrator plus/Vacufuge® plus, Eppendorf, Germany).

For the survey of cell metabolome changes with UHLC-HR-MS, *A. minutum* and *H. triquetra* were extracted with methanol or MeOH/EtOH/CHCl₃ (1:3:1) at 9 and 16 days of incubation, respectively.

3.4.2 UHPLC-HR-MS Parameters

The metabolic separation was performed onto a C18 column (100 × 2.1 mm, 2.6 µm) using a 14 min gradient of phase (2 % acetonitrile, 0.1 % formic acid in water) and acetonitrile phases (0.1 % formic acid in acetonitrile). Mass spectrometry was conducted in positive and negative-ion modes with a scan range of 100 to 1500 *m/z* at a peak resolution of 140 000.

3.5 Metabolic profiling in dinoflagellates-copepodamide interaction

For the toxin induction experiments, algal cells were treated with either copepodamides extracts or synthetic analog. Cultures were incubated in 2 ml Eppendorf tubes or 4 ml HPLC glass vials for 3 days. Different ages of inoculating cultures were assessed with cells either in the exponential or late growth phase (14 and 29 days, respectively). The initial cell count at the start of these experiments was also assessed, ranging from 50.000-195.000 cells·ml⁻¹. In total, five experiments were carried out in biological triplicates and one with five replicates.

3. Material and methods

3.5.1 Extraction methods and sample preparation

Dinoflagellates cells were extracted by sonication in an ultrasonic bath at room temperature for 10 min or with 3 freeze-draw cycles. The extraction of the cell cultures was carried out in filter funnel heads (glass beaker, PP funnel, seals from DURAN, Mainz, Germany) with filter disk with glass rim (DURAN, Mainz, Germany). GF/C-filters (24mmØ, pore size 4, glass edge, VWR International GmbH, US) were used.

The supernatants were transferred into corresponding screw caps (MACHEREY-NAGEL GmbH & Co. KG, Dueren, Germany) and dried with a concentrator (Concentrator plus/Vacufuge® plus, Eppendorf, Germany).

The copepodamides extract or the synthetic analog were dissolved in methanol and tested at 1 nM final concentration by adding 50 µl of stock solution to each tube, then dried under argon according to Selander *et al.* The controls consisted of adding 50 µl of methanol then drying the samples under argon.

3.5.2 UHPLC-HR-MS Parameters

The cultures were centrifuged for 15 min at 3000 rpm, supernatants removed and cells were extracted with 70 µl of acetic acid in mqWater (0.05M). Here, two extraction processes were assessed, either 5 min in an ultrasonic bath or 3 freeze-draw cycles. The extracts were then centrifuged for 20 min at 12 000 g and 50 µl of supernatant were transferred to new vials. The metabolic separation was assessed on three different columns for polar compounds (C8, RP synergic, ZIC-HILIC) using a 14 min gradient of aqueous (2 % acetonitrile, 0.1 % formic acid in water) and acetonitrile phases (10% water, 5 mM ammonium acetate).

3.6 Data analysis and statistic

The software Xcalibur Version 3.0.63. (Thermo Fischer Scientific Inc., Germany) was used to analyze the UHPLC-HR-MS data and the raw data were analyzed with CompoundDiscoverer™ (version 3.0, Thermo Fisher Scientific, USA) to explore further the identity of the signals and export list of metabolites (chemical formula, *m/z*, retention time) as an excel list. The data records in the Excel list were sorted manually; therefore all data records without a formula were removed. Furthermore, the data was converted into a comma-separated format (.csv). The remaining data records with the new .csv formatting

3. Material and methods

were then processed by the online software MetaboAnalyst 4.0 (<https://www.metaboanalyst.ca/>). For this purpose, the data sets were uploaded as "Samples in columns (unpaired)" and then normalized sample-specifically via data transformation and data scaling. T-test, ANOVA and Volcano plots were used to identify significant differences between untreated and treated cells.

After complete processing with MetaboAnalyst 4.0, the significant metabolites determined were tested with SIRIUS. The available MS/MS data were compared with the PubChem database to determine the probability of which substance they were. MS² spectra are compared with this PubChem database by using the CSI:FingerID tool which is integrated into the SIRIUS software. By isotope pattern analysis, SIRIUS recognizes molecular formulas and provides information on the fragmentation of metabolites by generating fragmentation trees. MS/MS data from putative lipids were compared by using the online database LipidMaps (<https://www.lipidmaps.org/>).

4. Results & Discussion

4.1 Growth condition

The effect of silicate depletion and increased salinity was assessed on the growth of the healthy and infected dinoflagellate *A. minutum*. Healthy cells were incubated in Penzé medium, made of seawater sampled from the original location at low salinity of 27 g·L⁻¹ (27 PSU) and F/2 Guillard's medium with a salinity of 35 g·L⁻¹ (35 PSU). The effect of silicate supplementation was assessed with the addition of 15 mg·L⁻¹ of sodium metasilicate to the F/2 medium. In order to determine the influence of the culture medium on infected cells, *A. minutum* was subsequently infected with 250 µL *Parvilucifera rostrata*. Cellular densities were counted every three or four days for three weeks. The initial concentration of the untreated cells was 100 cell·mL⁻¹ and that of the treated cells 90 000 cell·mL⁻¹.

4.1.1 Effects of nutrients supplementation on the growth of dinoflagellate

The cultivation in Penzé medium allowed the recovery of the maximum cell density on day 3 and the stationary phase was reached very quickly. Nevertheless, it can be presumed that the growth rate over the entire period of 20 days is statistically significantly lower for the penzé medium. In both F/2-mediums the cells need a longer time for growth, their maximum cell density cannot be determined within a time frame of 20 days. But there was also a difference between the two F/2 media where it becomes clear that the cells grow better without the addition of silicates. This becomes clear due to the continuously higher cell density in the F/2 medium without silicate compared to the F/2 medium with silicate. A comparison of the growth rates of the cells showed no statistically significant difference (ANOVA, p-value = 0.255) in the selection of the medium. The growth rate was calculated accordingly according to Strom *et al.*¹⁰⁹

4. Results & Discussion

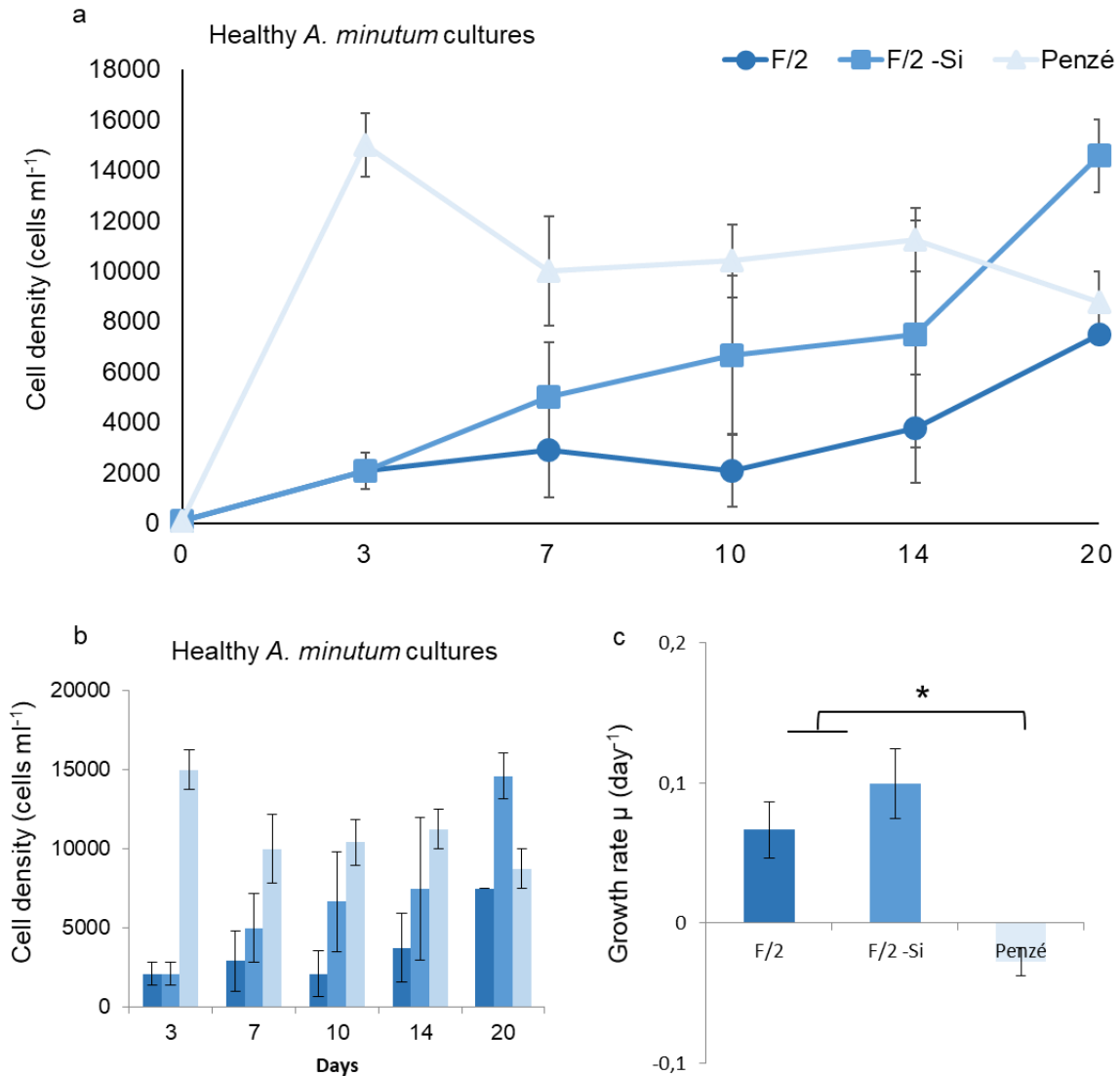


Figure 6 a) Growth curves of healthy *A. minutum* grown in three different culture media (F/2 with silicate supplementation, F/2 -Si no silicate supplementation, Penzé medium) either as untreated (healthy cultures). b) Cell density and c) growth rates of *A. minutum* grown in three different culture media (F/2 with silicate supplementation, F/2 -Si no silicate supplementation, Penzé medium). The average values of the growth rates are shown along with the standard deviation. A Student's test found statistical significance between the F/2-mediums and Penzé medium (* for P-value < 0.05).

4. Results & Discussion

The exponential growth increase combined with a lag phase at the beginning at a higher salinity was already observed in earlier experiments with *A. minutum*.¹¹⁰ Similarly, other studies have shown that the growth rate rises with an increase of 20 PSU up to 40 PSU.¹¹¹ But most of the strains of *A. minutum* have an increased growth rate of only up to 30 PSU.¹¹² An exception is the Strain AM89BM, which was isolated from the Bay of Morlaix, Brittany, France, and has already been observed. The *A. minutum* strain RCC3008, which was used for this thesis, was isolated from Roscoff, which is located near the Bay of Morlaix.¹¹³ Thus, a similar habitat can be assumed for both strains, which could explain the increased tolerance to salinity. This is also confirmed by the statistically significant difference between 27 PSU of the Penzé medium and 35 PSU of the F/2 medium.

4.1.2 Effects of nutrient supplementation on the growth of infected cells with *P. rostrata*

Since mainly infected dinoflagellates were treated during this thesis, it was important for us to find a suitable medium for this as well. For this reason, the first test series was repeated with *A. minutum*. During the repetition, however, the dinoflagellates were additionally infected with *P. rostrata*.

For the determination of the growth curve and growth rate of the treated cells, the total cell count of healthy and infected cells was determined. Regardless of the medium, the cell density decreased rapidly in the first three days, reaching another growth boost until the 10th day and then decreasing continuously over time. There were no statistically significant differences in cell density between the media as also for the growth rate.

4. Results & Discussion

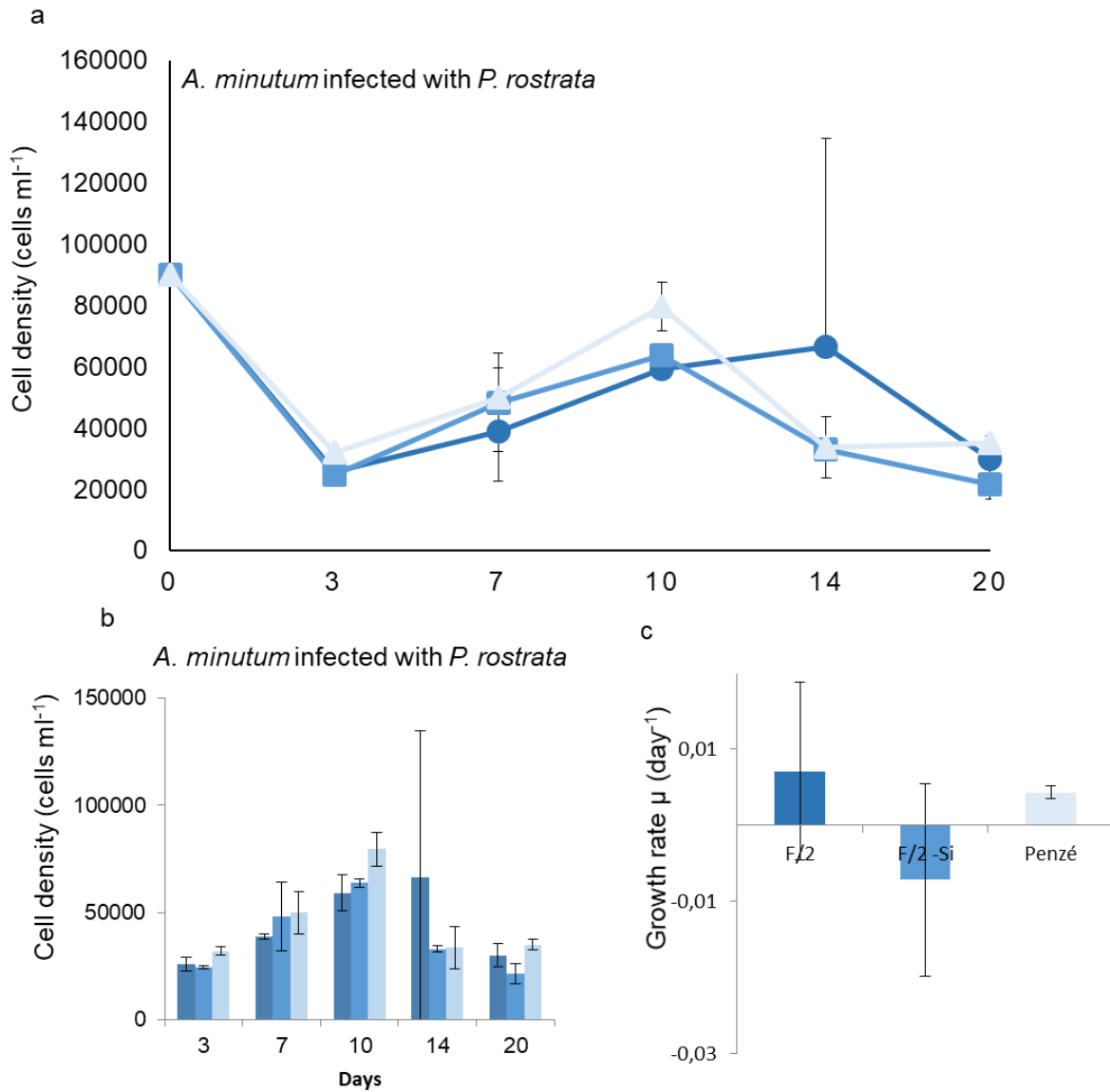


Figure 7 a) *A. minutum* treated with cells infected by *Parvilucifera rostrata*. The average values of the cell densities are shown along with the standard deviation. N = 3 for both experiments. b) Cell density and c) growth rates of *A. minutum* grown in three different culture media (F/2 with silicate supplementation, F/2 –Si no silicate supplementation, Penzé medium) for cells infected by *Parvilucifera rostrata*. (one way ANOVA, * for p-value < 0.05).

4. Results & Discussion

In order to study the factors influencing the parasite disease, the infection rate was calculated for all mediums. To determine the infection rate, all infected cells were used which can be identified by microscopy according to Garcés *et al.*⁸¹

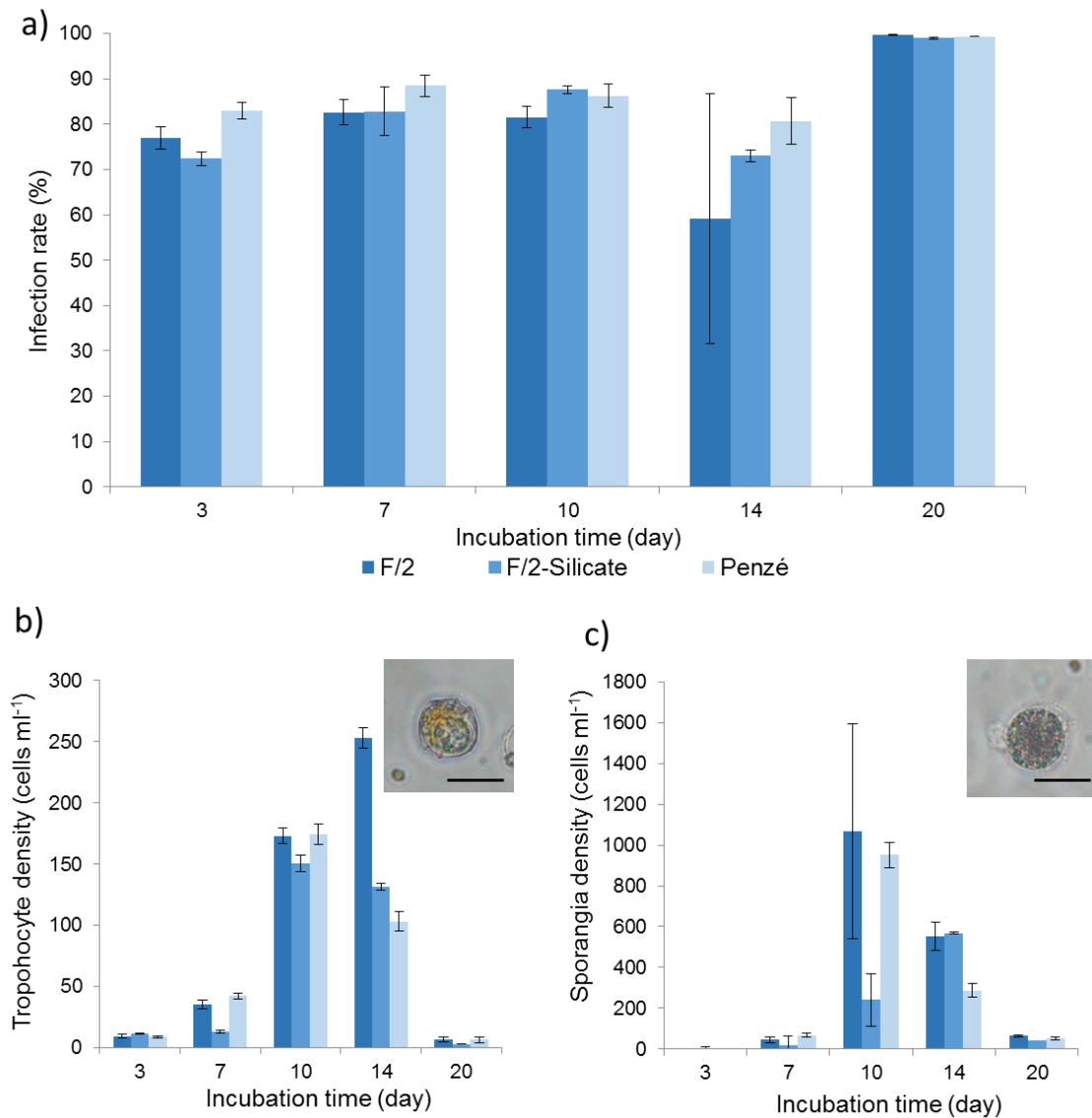


Figure 8 a) Infection rate of *P. rostrata* infecting *A. minutum* evaluated in three different culture media (F/2 with silicate supplementation, F/2 –Si no silicate supplementation, Penzé medium) Cell counts of parasitic trophocysts (b) and sporangia (c) in infected *A. minutum* cultures in three different culture media (F/2 with silicate supplementation, F/2 –Si no silicate supplementation, Penzé medium). Representative microscopy pictures from Alacid *et al.* Scale bars equal 20 μm.⁸⁵

4. Results & Discussion

Already after 3 days, a high infection rate for all media was observed. No statistically significant difference ($p > 0.05$) was seen for the infection of cells grown in the different mediums. A closer look at the infections revealed that the highest concentration of trophocysts and sporangia was detected between day 10 and day 14. Until the 7th day, mainly cells were counted to identify the infection, which lost their motility and were still not in the stage of the trophocysts. It is important to mention that on the 20th day the infection had progressed so far that only the number of dead cells could be used to identify the infection.

As a conclusion, it can be suggested that *A. minutum* can grow independently of salinity, but there is an increase in cell concentration during the first few days for Penzé with lower salinity (Figure 6a). This is important for the further test series, where a high concentration of the cells with a short incubation period of 3 days is desired. For the use of cultures from 14 days where an increased cell density is desired, the F/2 medium is more suitable without the addition of silicate. For a more accurate growth rate and a good differentiation between both F/2 media, investigations should go beyond the 20th day. Considering the growth rate of the infected cells, the hypothesis can be made that *A. minutum* can be infected faster in a medium with low salinity, resulting in a decrease in the growth rate (Figure 7c). This would have to be tested more closely in a series of experiments with different salt concentrations of a medium. Why salinity matter so greatly on the infection rate should also be further studied.

For further experiments where infected cells are to be examined, the selection of the medium is not selective and all media can be used, as both the cell density over 20 days and the growth rate does not allow any significant difference.

Another result of this experiment is that the concentration of trophocytes and sporangia is highest between the 10th and 14th day (Figure 8 b/c). This information is important for the correct timing of possible experiments in the future, e.g. to analyze the metabolites of these two infection phases.

4. Results & Discussion

4.2 Investigations of cellular changes upon parasitic infection

In order to better understand the interaction between dinoflagellates and parasites, it is important to understand the changes in physiology and metabolites during infection. For this purpose, the virulence of the parasite strains of *P. rostrata* and *P. infectans* against the hosts *A. minutum* and *H. triquetra* was investigated. Both dinoflagellates are from the Roscoff Culture Collection.

4.2.1 Growth rate of infected non-toxic and toxic dinoflagellates

To investigate the changes in growth rate, the non-toxic dinoflagellate *H. triquetra* and the toxic dinoflagellate *A. minutum* were infected with parasitoid *Parvilucifera rostrata* and *Parvilucifera infectans* for 16 (HT) and 9 (AM) days, respectively. The infection was identified by microscopy as described in the literature.⁸¹

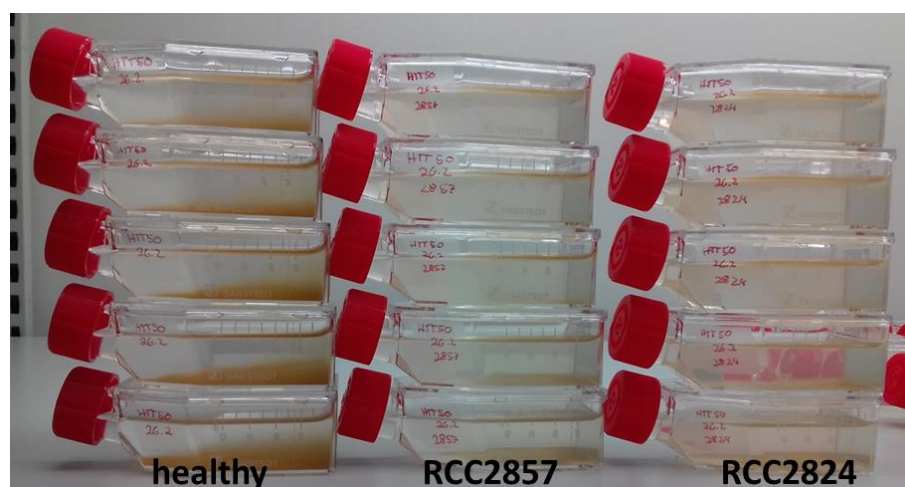


Figure 9 Culture of treated and untreated *H. triquetra* after 16 days of incubation

A growth rate for both dinoflagellates was determined in the healthy and infected state, with *P. rostrata* and *P. infectans*. For this purpose, 1 mL of each cultivation was removed and the cell count was determined as usual using the Neubauer chamber. The first difference between the two infected dinoflagellates is already noticeable during cell concentration determination. For *A. minutum* no addition of Lugol is necessary for counting the infected cells since the infection has progressed so far that the cells are not moving anymore. A difference can be observed at *H. triquetra*, where, as with healthy cells, 10% Lugol had to be added. Lugol is used to fix the cells and to simplify the counting of the cells.

4. Results & Discussion

For *H. triquetra*, no statistical difference was found by one-way ANOVA between healthy and infected cells for the growth rate. However, there is still a statistically significant difference ($N = 5$, p -value = 0.008) between the infected cells with *P. rostrata* and *P. infectans* for *H. triquetra* confirmed by a t-test.

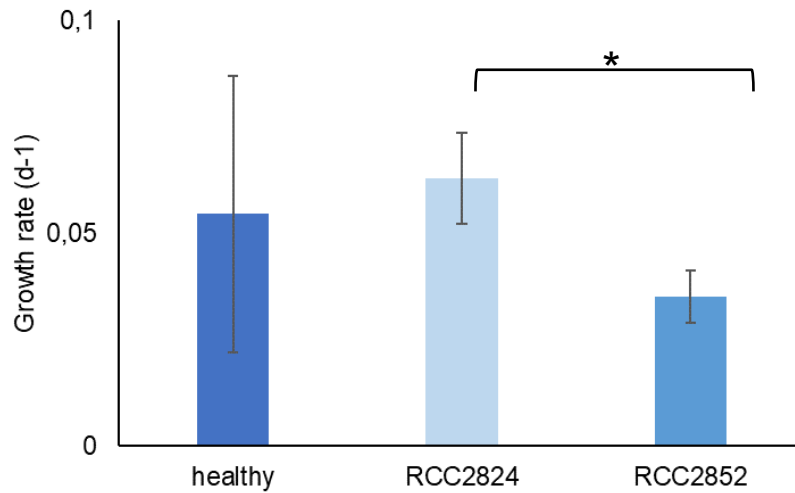


Figure 10 Growth rate of *H. triquetra* grown in Penzé medium and treated with *P. rostrata* (RCC2852) and *P. infectans* (RCC2824)

For *A. minutum*, a statistical difference ($N = 5$, p -value = 0.001) between infected and healthy cells can be determined by one way ANOVA but no statistically significant difference ($N = 5$, p -value = 0.093) exists between the infected cells.

4. Results & Discussion

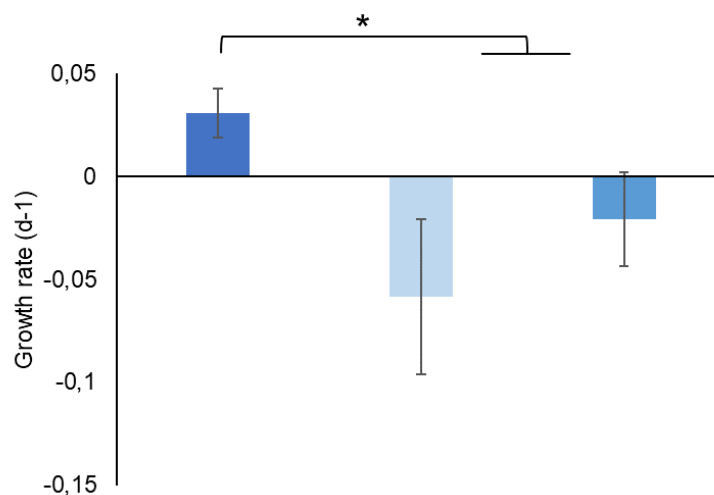


Figure 11 Growth rate of *A. minutum* grown in Penzé medium and treated with *P. rostrata* (RCC2852) and *P. infectans* (RCC2824)

Since the standard deviation of healthy cells for *H. triquetra* is very large, no exact statement can be made about a change in the growth rate of infected cells (Figure 10). However, it should be noted that a comparison of the motility between infected cells of *H. triquetra* and *A. minutum* shows a significant difference. The presence of motility in most infected cells of *H. triquetra* indicates that this non-toxic dinoflagellate is less sensitive to both parasitoids. This also supports the observation that a longer incubation period of 16 days is necessary for *H. triquetra* to decimate the whole population. For *A. minutum* the expected effect has occurred according to the literature and has a lower growth rate for the infected cells (Figure 11).¹⁰⁶ *A. minutum* has a high sensitivity to both parasitoids.

4.2.2 Metabolic investigation of *H. triquetra* and *A. minutum*

To investigate a variation in metabolites in treated and untreated cells endometabolome, the extracts were analyzed by UHPLC-MS/MS. The total yield of the metabolites (formula, m/z , retention time) of the analysis was obtained from raw data processing performed in Compound Discoverer.

The analysis of *H. triquetra* extracts yielded 732 metabolites (formula, m/z , retention time), among 301 were found statistically significant by fold change analysis (p -value < 0,05) with MetaboAnalyst in extracts of infected *H. triquetra* with *Parvilucifera rostrate*/*Parvilucifera*

4. Results & Discussion

infectans vs. healthy cells of them. The analysis of *A. minutum* extracts yielded 189 metabolites (formula, m/z , retention time), among 6 were found statistically significant by fold change analysis (p -value $< 0,05$) with MetaboAnalyst in extracts of infected *A. minutum* with *Parvilucifera rostrata* or *Parvilucifera infectans* vs. healthy cells of them. In order to determine the distribution of the up- and downregulated metabolites in the different treatments, a volcano plot was also created for all results. All ions, for *A. minutum* and *H. triquetra*, were detected in positive polarity.

The reproducibility and analytic robustness of the UHPL-MS/MS were assessed by comparing the LC-MS profiles of the QC samples (Fig 12a). The total explained the variance of 89.1% of metabolic changes between healthy and infected cells of *H. triquetra* could be significantly discriminated (Fig 12b). Likewise, a discrimination of the metabolites of the different parasitoids is possible.

The metabolic changes between healthy and infected cells in *A. minutum* were not as clear as those for *H. triquetra* (Figure 13). The total explained variance of 42% of metabolic changes between healthy and infected cells does not allow for clear significant discrimination for *A. minutum*. The identity of these selected ions was confirmed by spectral similarity search in PubChem with using SIRIUS and CSI:FingerID (Table 3).

4. Results & Discussion

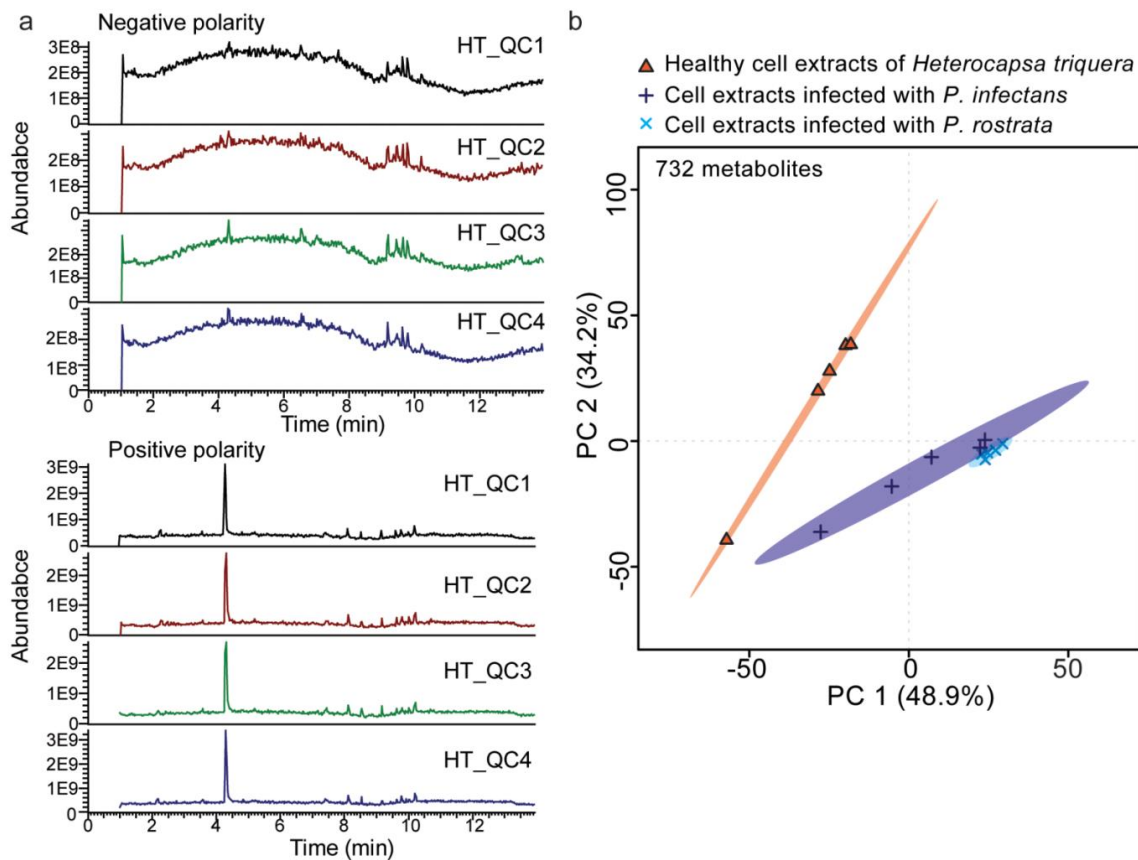


Figure 12 Metabolic investigation of dinoflagellate *H. triquetra* during infection by parasites *Parvilucifera* spp. a) Total ions chromatograms depicting the pool samples analyzed four times through the UHPLC-MS/MS run in positive and negative polarities. b) Significant changes in the metabolic content of *H. triquetra* cells healthy or infected either by *P. rostrata* or *P. infectans*.

4. Results & Discussion

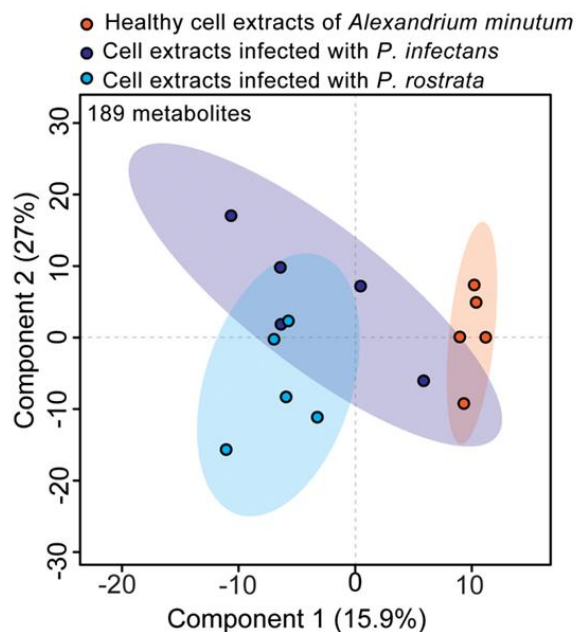


Figure 13 Significant changes in metabolic content of healthy or infected cells of *A. minutum* found by PLS-DA analysis.

For *H. triquetra*, 6 classes of the corresponding metabolites were identified, but only one for *A. minutum*. All identified metabolites were found also in the loading plot of PCA and PLS-DA to discriminate the significant metabolites but not as the top of the VIP features. The limited number of metabolites found in *A. minutum* is among other things since the concentration of the samples was too low. This was corrected in further experiments with *H. triquetra*. Furthermore, only methanol was used for the extraction of *A. minutum* and no mixture of MeOH:EtOH:CHCl₃, which makes another essential difference as both are polar but MeOH is protic and CHCl₃ is aprotic. For this reason, the results of the two dinoflagellates cannot be compared.

4. Results & Discussion

Table 3 Selected metabolites from one-way ANOVA test with a proposed identity (class), retention time (RT), observed ion traces and identity score (CSI %) found by MS/MS spectral similarity search with the public database. **In bold** is one of the most significant metabolites discriminating infected from healthy extracts of *A. minutum*. (Up-regulated in: *all treated cells; **RCC2857; ***healthy cells)

Chemical Formula	RT (min)	m/z [M+H] ⁺	CSI score (%)	f-value (p-value < 0.05)	InChIKey	Class
C₃₀H₄₈O₂*	9.4	441.3747	60.7	27.155	LGDWOJXZVCOMEAMOCJTXXKSA-N	Sterol derivate
C₉H₁₅N₃O₂S***	2.3	229.08844	40.9	19.426	AZGGKEWAAASMRXUHFFFAOYSA-N	Cysteine derivate
C₃₅H₃₆N₄O₆*	8.9	608.26282	58.0	64.084	KECOXFKVIHSIBOUHFFFAOYSA-N	Porphyrin
C₃₀H₅₀O₂*	10.6	443.33286	63.7	19.739	WXSZYFSBLQQISHCZSACIGHSA-N	Sterol derivate
C₂₃H₄₇O₆P***	10.7	450.31020	44.9	39.164	VFOWWTAPMOPOCJHSZRJFAPSA-N	cyclic chlorophosphate
C₂₇H₄₂O₂*	9.8	399.3229	58.9	51.091	ADIQUEDCGDLKDP-PWQYKKGWSA-N	Steroid derivate
C₂₁H₃₄O₄***	9.2	332.23472	66.7	9.547	WNCUAIVHPMNYAKLTKCOYKYSA-N	monoacylglyceride
C₆H₁₃NO₂**	1.2	131.09462	77.6	5.518	ROHFNLRQFUQHCHUHFFFAOYSA-N	Amino acid
C₁₀H₁₈N₂O₅**	1.8	246.12135	83.8	7.846	AQAKHZVPOOGUCK	Amino acid
C₂₂H₃₆O₃**	7.8	348.26617	61.2	10.271	NDZUVNRLCYRNGT	Lipid
C₆H₁₃NO₂**	1.3	131.09471	58.8	13.194	AGPKZVBTJJNPAGWHFBIKZSA-N	Isoleucin

Especially conspicuous are the sterol and steroid derivatives in the identified metabolites, as they only appear in the treated cells. This could be a first indication for the defense of the Dinoflagellates against the parasitoids. Microalgae, which also include dinoflagellates, form sterols for their function as membrane lipids but also as possible defense materials.¹¹⁴ According to Ines Yang *et al.*, it was shown that the concentrations of putative steroid oxidoreductase superfamily in toxic strain are 2.9 to 4.5 times higher than in non-toxic strains

4. Results & Discussion

of *A. minutum*.¹¹⁵ However, *H. triquetra* is not a toxic dinoflagellate, but the hypothesis can be made that the increased concentrations of sterols derivatives of the infected cells of *H. triquetra* still serve as a defense against the infection, possibly a similar one as for toxic dinoflagellates. Since a low concentration of steroids is also present in the healthy cells, it can also be assumed that these are not metabolites of the parasitoids. For the steroid C₃₀H₅₀O₂ with the highest CSI-score of 63.7% for all sterols (MS spectra are seen in appendix), it can be proved by literature that this compound has cytotoxic and antiviral activity.¹¹⁶ An expected higher concentration of sterols was not found in the toxic alga *A. minutum*, which can be explained by the use of another solvent. Only polar methanol was used for *A. minutum*, which cannot dissolve the mostly non-polar sterol derivatives at all.

Moreover, other dinoflagellates such as *Amphidinium carterae* can change their amino acid and carbohydrate metabolism in the event of nitrogen starvation to induce oxidative stress.¹¹⁷ In this step to ensure survival, an elevated concentration of 3-hydroxyacyl-CoA-dehydrogenase (HADH) was detected. These HADHs are involved in amino acid metabolism and degrade the amino acids valine, leucine and isoleucine. Based on this, it could be assumed that similar enzymes are produced for defense against the stress of an infection, which leads to the formation of free amino acids with leucine, valine or isoleucine as the C- or N-terminus. Looking at the upregulated metabolites of *H. triquetra* and *A. minutum*, an increased concentration of these amino acids can be observed in the infected cell. Especially for *H. triquetra*, a high CSI score of the corresponding amino acids was identified. This could be a further indication that the dinoflagellates *H. triquetra* tries to defense the infection. To verify this hypothesis, an inhibitor of HADH can be used for further experiments in order to subsequently check whether a further increased concentration of amino acids is detected.

4. Results & Discussion

4.3 Toxin induction assays

While not all strains of *A. minutum* can produce toxins, their expression sometimes might be silenced under unchallenged conditions. For this purpose, bioactive lipids copepodamides produced by the predators copepods were used to regulate and increase the toxin expression in *A. minutum*.

The effects of copepodamides extract and a synthetic analog (Figure 14) were assessed on algal growth and metabolic production, at the final concentration of 1 nM per sample. Based on the protocol of Selander *et al.*, we carried out a series of experiments with different dinoflagellates strains (Table 1) and performed an extraction to build an extractotheque.⁹² The extracts were investigated by UHPLC-MS/MS-based on a protocol of Rassignoli *et al.*¹¹⁸

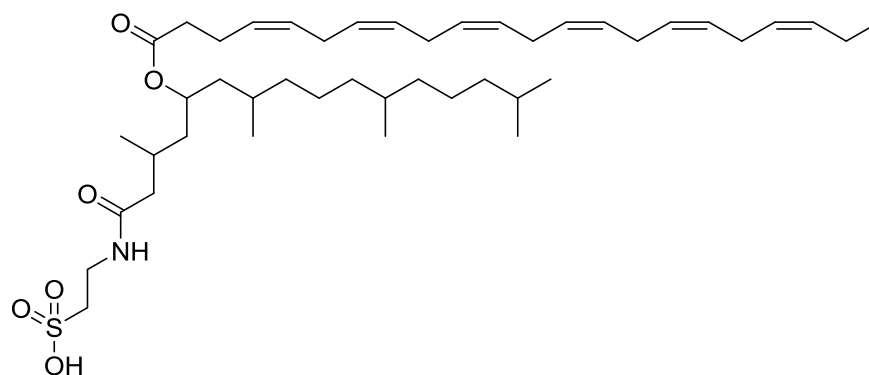


Figure 14 Chemical structure of the synthetic analog (unpublished results, Ph.D. Marino Wirgenings).⁹¹

4.3.1 Effect of copepodamides on algal growth performance and infection

The influence of copepodamides on cell growth was determined. The already known strain RCC3008 of *A. minutum* from previous experiments was used for the first series. First, the influence of extracts mixture copepodamides on the growth of dinoflagellates was investigated. For this purpose, a method according to Selander *et al.* was further elaborated in which some parameters were changed. The number of replicas used can be found in the tables below.⁹¹

4. Results & Discussion

Table 4 Metadata of the toxin induction experiments with synthetic copepodamides

	Test 1	Test 2	Test 3	Test 4
Initial cell count (cell·mL⁻¹)	50.000 (RCC3008)	195000 (refreshed with 1/2 volume Penze medium)	88750 (RCC3008)	5000 (HT150), 6250 (RCC2663), 8750 (RCC1490), 10000 (RCC2672), 10000 (RCC3008)
Age of initial culture (days)	14	26	29	22
Volume of culture (mL)	1	1	2	5
Number of replicates	3	3	5	4
Centrifugation	15 min 2000 rpm	15 min 3000 rpm	15 min 3000 rpm	15 min 12000 rpm
Volume of extraction with acidic water (0,05M Acetic acid) (µl)	70	70	100	70
Extraction	5 min in an ultrasonic bath at RT	10 min in an ultrasonic bath at RT	5 min in an ultrasonic bath at RT	3 freeze draw steps
Centrifugation	12 000 g 20 min	12 000 g 20 min	12 000 g 20 min	10 min 3000 rpm
Volume of supernatant sampled (µl)	20	20	50	50
Volume of acetonitrile added (µl)	50	50	100	70

Table 5 Metadata of the toxin induction experiments with natural extracts copepodamides

	Test 1	Test 2
Initial cell count (cell·mL⁻¹)	132500 (RCC3008)	187 000 (RCC3008)
Age of initial culture (days)	14	16
Volume of culture (mL)	1	1
Number of replicates	3	3
Centrifugation	15 min 3000 rpm	15 min 3000 rpm
Volume of extraction with acidic water (0,05M Acetic acid) (µl)	100	100
Extraction	5 min in an ultrasonic bath at RT	5 min in an ultrasonic bath at RT
Centrifugation	12 000 g 20 min	12 000 g 20 min
Volume of supernatant sampled (µl)	50	50
Volume of acetonitrile added (µl)	50	50

4. Results & Discussion

Due to the short incubation period of 3 days, only the cell density on day 0 and day 3 was compared, because a significant growth rate requires more time.

For half of the test series with the extract mixture copepodamides, a statistically significant difference between untreated cells could be determined. A similar situation was observed for the synthetic copepodamide, two out of three test series showed a statistically significant difference between untreated and treated cells. However, it is striking that the difference between treated and untreated cells of the extracts mixture copepodamide is significantly wider.

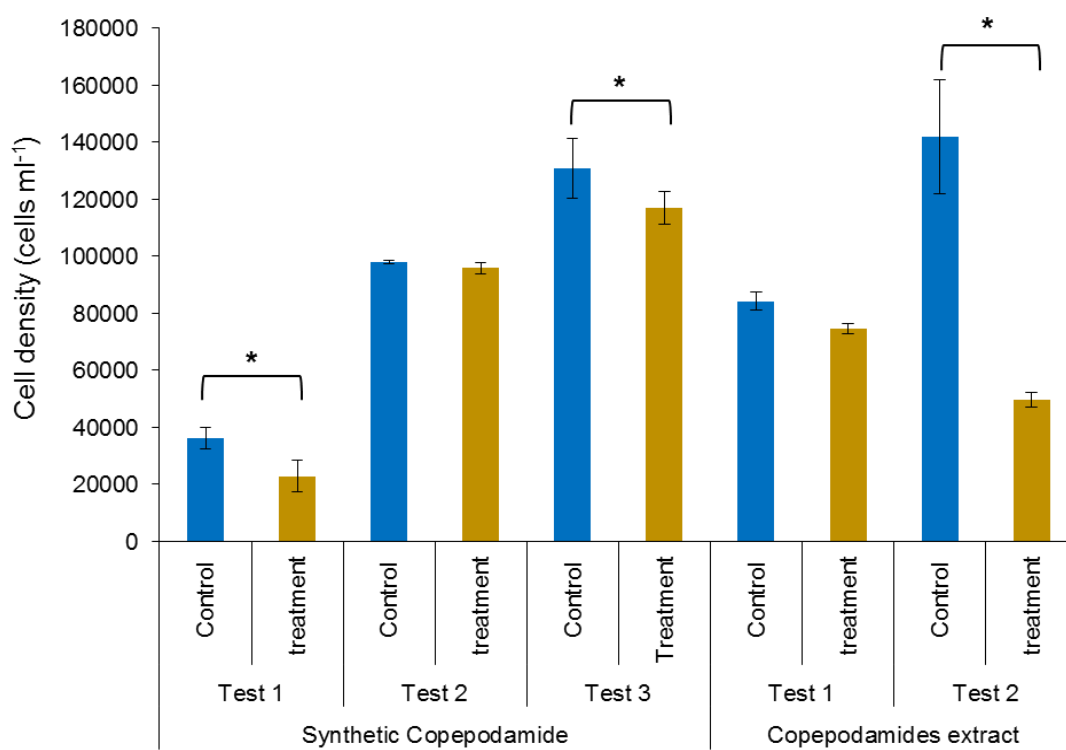


Figure 15 Cell densities of *A. minutum* RCC3008 treated with 1 nM of extracts mixture of copepodamides, synthetic copepodamide or methanol. The average values are shown along with the standard deviation. A Student's test found statistical significance between control and treatment (* for P-value < 0.01), but not for all independent experiments.

Afterward, the influence of copepodamide on other strains of the toxic *A. minutum* was tested. For this purpose, the strains RCC2663, RCC1490, RCC2679 and RCC3008 were used. The influence on the non-toxic dinoflagellate *H. triquetra* was also investigated. In order to

4. Results & Discussion

obtain solid results, 5 replicas were used for each test series. A larger volume was also used, as part of the cultures are needed for a further experiment. Only a new synthetic copepodamide with the same structure was used for this test series. It should also be noted that for the extract for this series, unlike the others, three freezing stages were performed. First, it can be seen that the treatment with synthetic copepodamide does not affect *H. triquetra* so much. However, the strains of *A. minutum* are different (Figure 16). All show a statically significant decrease in cell density in the treated cells. Especially for the strains RCC2663, RCC2672 and RCC3008 ($p < 0.003$).

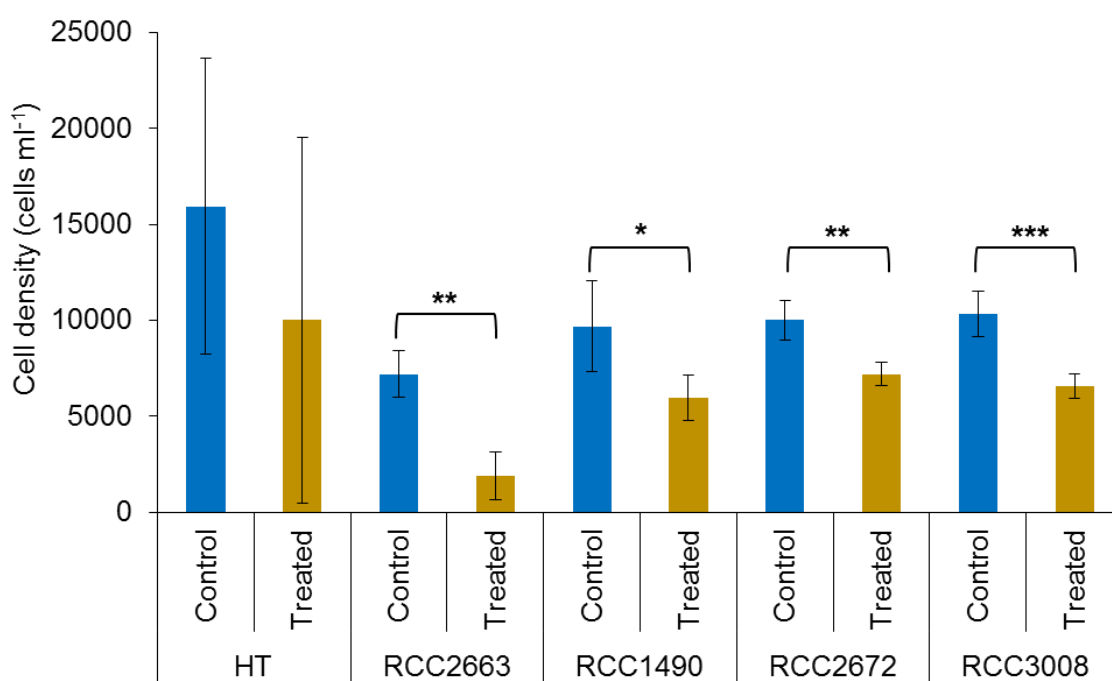


Figure 16 Cell densities of *A. minutum* (RCC2663, RCC1490, RCC2672, RCC3008) and *H. triquetra* (HT) grown for 2 days with synthetic copepodamide or with methanol (0.1%). The average values are shown along with the standard deviation. A Student's test found statistical significances for *Alexandrium* cells treated with copepodamide and those with methanol (N = 4, for RCC2663 $t = -6.140$ P-value < 0.001 , for RCC1490 $t = -2.828$ P-value = 0.03, for RCC2672 $t = -4.700$ P-value = 0.003, for RCC3008 $t = -5.555$ P-value = 0.001).

After determining the cell density, 2 ml of the culture was subsequently infected with 10 μ L *P. rostrata*. The growth rate was then determined after a further 3 days. It can be seen that the

4. Results & Discussion

infection does not make a statistically significant difference in the growth rate between infected and non-infected cells (Figure 17).

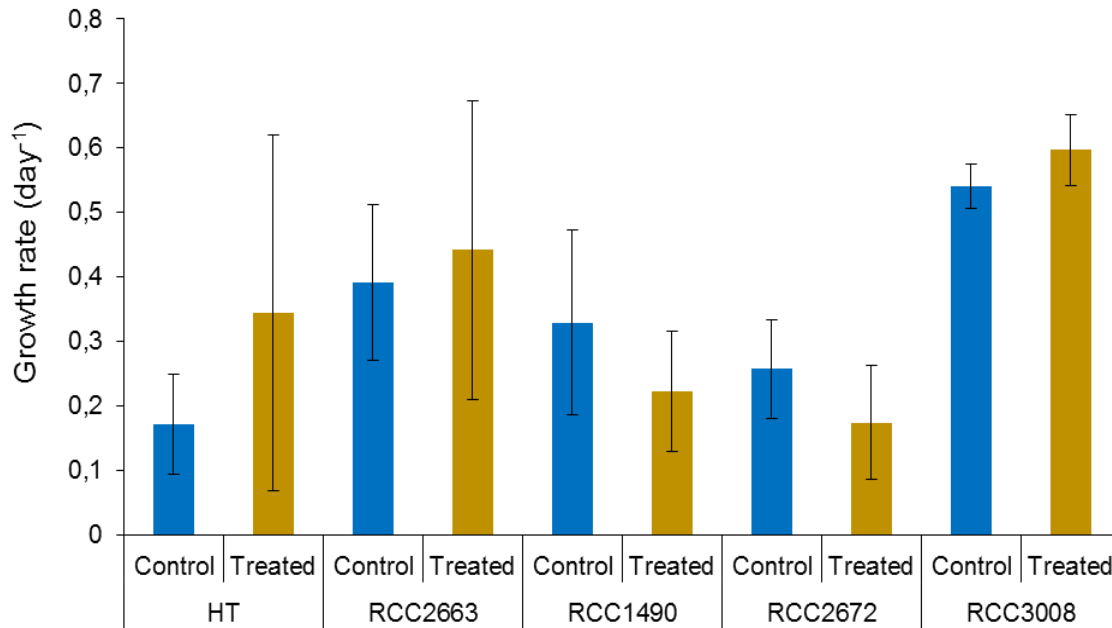


Figure 17 Growth rates of *A. minutum* (RCC2663, RCC1490, RCC2672, RCC3008) and *H. triquetra* (HT) grown for 6 days in Penzé medium and were infected with *P. rostrata* 3 days after treatment with copepodamies. The average values are shown along with the standard deviation. A Student's test did not found statistical significance between copepodamide and methanol treatment (N = 4, P-value = 0,201).

Regarding the first test series exclusively with *A. minutum* RCC3008, the following assumptions can be made that the difference in Test 2 of the treatment with the synthetic copepodamide could be explained by the fact that new fresh medium was added here. By adding new nutrients the cells of the untreated and treated dinoflagellates may react differently than in the other test series. For this reason, the addition of fresh medium must be avoided in the future. The very different results for copepodamides extract might be since the stability of the substances in methanol is not guaranteed overtime.

Conclusively, it can be said for the cell density for the test series with the dinoflagellates *H. triquetra* and *A. minutum* that a low cell density can be observed in the treatment of the

4. Results & Discussion

cells after 3 days of incubation. This effect is not always reproducible, which motivates further experiments to confirm it.

Another interesting observation is that the growth rate of untreated cells of the *A. minutum* strain RCC3008 (Chapter 4.2) deviates from the new results. After treatment with Copepodamides for 3 days, statistically, significant reductions in the growth rate due to infection with *P. rostrata* are no longer detectable. It can, therefore, be assumed that the treatment with Copepodamides contributed to a better defense of the dinoflagellates *A. minutum* against the parasitoids.

4.3.2 Cell metabolome investigations upon treatment with copepodamide

To investigate possible metabolites that might be involved in the increased resistance, all test series were extracted and analyzed by UHPLC-MS/MS.

The UHPLC-MS analysis of *A. minutum* extracts on C8 column for Test 1 for the treatment with the synthetic copepodamide yielded 234 metabolites (formula, m/z , retention time), among 76 were found statistically significant by fold change analysis (p -value < 0,05) with MetaboAnalyst in extracts of treated *A. minutum* with synthetic copepodamides vs. untreated cells of them. The identity of these selected ions for all test series was confirmed by spectral similarity search in PubChem with using SIRIUS and CSI:FingerID (Table 6). The reproducibility and analytic robustness of the UHPL-MS/MS were assessed for test series earlier. The total explained the variance of 94.1% of metabolic changes for the test between untreated and treated cells of *A. minutum* could be significantly discriminated (Fig 18).

4. Results & Discussion

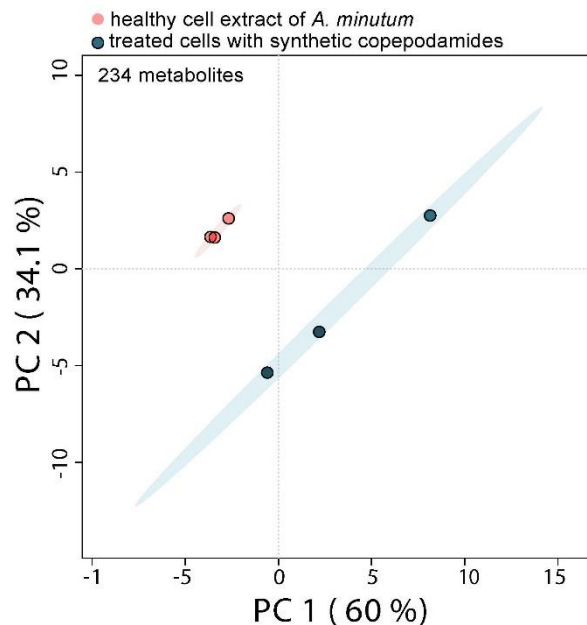


Figure 18 Significant changes in metabolic content of untreated or treated cells of *A. minutum* found by PCA analysis.

Only 11 metabolites could be further investigated by tandem mass spectrometry (Table 6). They are also among the most important metabolites found in the PCA loading plot. The detected metabolites with the highest CSI score are mainly amino acids, which all have a leucine unit at the C- or N-Terminus. Thus similar amino acids could be found in the treated cells as in the treatment with the parasites (chapter 4.2). This could be a further indication that the enzymes are involved in the defense mechanisms and also supports the hypothesis that the concentration of HADH increases toxin production in dinoflagellates. However, there are no saxitoxins or components of their biosynthesis to be found in statistically significant metabolites.

4. Results & Discussion

Table 6 Selected metabolites from one-way t-test with a proposed identity (class), retention time (RT), observed ion traces and identity score (CSI %) found by MS/MS spectral similarity search with the public database (They are all up regulated in treated cells)

Chemical formula	RT (min)	m/z [M+H] ⁺	CSI score %	t-value (p-value < 0.05)	InChIKey	Class (compound name)
C ₁₄ H ₁₉ NO ₂	2.8	234.1481	53.2	0.0012181	QMLWOUUGKNJFEK-UHFFFAOYSA-N	4-phenylpiperidine derivative
C ₂₄ H ₄₃ N ₂ O ₁₀ P	2.5	578.6413	37.5	0.0019307	ORFOEWTUUPUANF-ONRMWIAXSA-N	Organophosphate
C ₁₁ H ₂₂ N ₂ O ₃	2.8	237.7962	92.2	0.0062662	MDSUKZSLOATHMH-VEDVMXKPSA-N	Amino acid
C ₁₅ H ₂₉ N ₃ O ₄	3.2	337.4801	78.9	0.0061347	DYWZQNMGYPYXVNS-SRVKXCTJSA-N	Amino acid
C ₁₅ H ₂₂ N ₂ O ₃	3.2	287.2148	94.8	0.001736	KFKWRHQBZQICHA-ZGTCLIOFSA-N	Amino acid
C ₁₃ H ₂₀ N ₂ O ₅	2.0	285.1439	40.9	9.5803E-4	ZAZQCRXGPMAXTI-UHFFFAOYSA-N	Furoic acid derivatives
C ₁₀ H ₁₃ N ₅ O ₄	1.2	268.1037	96.7	7.5232E-4	OIRDTQYFTABQOQ	Adenin derivative
C ₉ H ₁₈ N ₆	1.1	212.5079	59.0	5.57E-4	BYRAQZROWBQUAH-UHFFFAOYSA-N	guanidine derivatives
C ₁₄ H ₂₇ N ₃ O ₄	2.9	302.2065	78.3	0.0082241	UXBZYLSMYOATLH-DCAQKATOSA-N	Amino acid
C ₁₅ H ₁₆ O ₅ S*	4.6 4.6	307.0646 [M-H] ⁻	54.9	4.6721E-5	FNUMGMFTOFJQDG-VIFPVBQESA-N	Organosulfate
C ₁₃ H ₂₄ N ₂ O ₉	3.3	355.1626	48.9	0.022562	AENNDQVVQAPGDH-BJKCNMQESA-N	Lysine derivatives

In order to investigate the metabolites of the test series with natural copepodamides extract, only Test 1 could be analyzed by MetaboAnalyst. No static significant differences ($p > 0.05$) between treated and untreated cells could be detected with the T-test. Also, the PCA did not allow any variance between the two conditions. A differentiation could only be made by using the Volcano plot, for the yield of 160 detected metabolites the identification of one metabolite only resulted (Table 7). For this reason, no information about the p-value can be provided.

4. Results & Discussion

Table 7 Selected metabolites from one-way t-test with a proposed identity (class), retention time (RT), observed ion traces and identity score (CSI %) found by MS/MS spectral similarity search with the public database

Chemical formula	RT (min)	m/z [M+H] ⁺	CSI score %	Upregulation	InChIKey	Class
C ₁₀ H ₁₇ N ₃ O ₆ S	0.9	308.1958	89.6	Treated cells	RWSXRVCMGQZWBV-WDSKDSINSA-N	Amino acid

The identified metabolite for treatment with the extract of copepodamide mixture is glutathione. Glutathione has the main task of maintaining proper cell function and preventing oxidative stress in cells.¹¹⁹ Special antioxidative genes and proteins, such as glutathione oxidase and glutathione reduction, have already been discovered for the dinoflagellates *Symbiodinium*.¹²⁰ It can, therefore, be assumed that the increased concentration of glutathione in the treated cells might be a defense reaction protecting against oxidative stress. Another interesting observation on glutathione has been made regarding the involvement in the transformation of gonyautoxins to saxitoxins.⁶³

In conclusion, it could be demonstrated that for all identified metabolites both for the natural copepodamid extract and for the synthetic copepodadmine a significantly higher concentration of new metabolites could be detected in the treated cells. It can, therefore, be assumed that these metabolites are formed during oxidative stress or that they may support toxin production differently from the known biosynthesis.¹²¹

4.3.3 Method development for PSP toxin detections

Based on the fact that bioactive lipids copepodamide increase the toxin expression of *A. minutum* and did not occur in statistically significant metabolites, some MS spectra were used to the identification of different metabolites (Table 9) during both parasitoid infection and treatment with copepodamides.⁹¹

For this purpose, a method was developed by the use of UPLC-HR-MS and various columns (ZIC-HILIC, C8, synergy RP). C8 was used for all previous assays and no PSP toxins could

4. Results & Discussion

be detected. The investigations with ZIC-HILIC and Synergie RP columns were different. ZIC-HILIC separates polar and hydrophilic compounds particularly well, whereas the Synergie RP column is well suited for the separation of polar and non-polar mixtures. It can be seen that most signals for ZIC-HILIC occur between one and 2 minutes, for RP synergy between 0.5 and 1.2 minutes.

Table 9 Expected m/z of the PSP toxins in dinoflagellates *Alexandrium*. *** m/z detected in positive polarity with the ZIC-HILIC column. **In bold**, m/z detected in positive polarity with RP synergy.

Algal toxin	Chemical formula	Molecular weight	expected m/z for $[M+H]^+$	expected m/z for $[M-H]^-$
Saxitoxin***	C₁₀H₁₇N₇O₄	299.2865	300.1414	298.1258
Gonytauxin 2***	C ₁₀ H ₁₇ N ₇ O ₈ S	395.0853	396.0932	394.0775
decarbamoylsaxitoxin***	C₉H₁₆N₆O₃	256.2620	257.1356	255.1200
neosaxitoxin	C₁₀H₁₇N₇O₅	315.1285	316.1363	314.1207
Saxitoxin Keton	C ₁₀ H ₁₅ N ₇ O ₃	281.1230	282.1309	280.1152
Saxitoxin Oxime	C ₁₀ H ₁₆ N ₈ O ₃	296.1339	297.1418	295.1261
Gonyautoxin 5	C ₁₀ H ₁₇ N ₇ O ₁₁ S ₂	475.0421	476.0500	474.0343
Nyautoxin C3	C ₁₀ H ₁₇ N ₇ O ₁₂ S ₂	491.0371	492.0449	490.0292
Gonytauxin 5	C ₁₀ H ₁₇ N ₇ O ₇ S	379.3510	380.0982	378.0826
Gonytauxin 1	C ₁₀ H ₁₇ N ₇ O ₉ S	411.0802	412.0881	410.0725
STX Dihydrochlorid	C ₁₀ H ₁₉ Cl ₂ N ₇ O ₄	371.0870	372.0948	370.0791
Saxitoxin Methyloxim	C ₁₁ H ₁₈ N ₈ O ₃	310.1496	311.1574	309.1418
Saxitoxinacetat	C ₁₄ H ₂₅ N ₇ O ₈	419.391	420.1837	418.1680
Saxitoxin Diacetat	C ₁₄ H ₂₅ N ₇ O ₈	419.1759	420.1837	418.1680
Saxitoxin P-bromobenzenesulfonate	C ₂₂ H ₂₇ Br ₂ N ₇ O ₁₀ S ₂	770.9622	771.9700	769.9543
okadaic acid	C ₄₄ H ₆₈ O ₁₃	805.0029	805.4732	803.4561
okadaic acid tetramethyl ether	C ₄₈ H ₇₆ O ₁₃	860.5280	861.5358	859.5202

For ZIC-HILIC there are too wide peaks and a slight tailing. Furthermore, as with the RP synergy double peaks were observed. SXT (300.1409 m/z), NeoSXT (316.1359 m/z) and decarbamoylSXT (257.1352 m/z) could be detected at RT=0.8 min with the analysis on RP Synergie and the MS/MS spectra were recorded in the positive polarity (Fig 12). NeoSXT was found to have a significantly lower intensity and concentration than the other PSP toxins. SXT (300.1409 m/z) and decarbamoylSXT(257.1352 m/z) could also be detected with the Synergie

4. Results & Discussion

RP column, additionally, MS/MS spectrum for GXTII (396.0932 m/z) with positive polarity was possible, but no library spectra were available at the time of analysis. Compared to the ZIC-HILIC a more efficient separation over the retention time is possible, even if it is very close for all toxins.

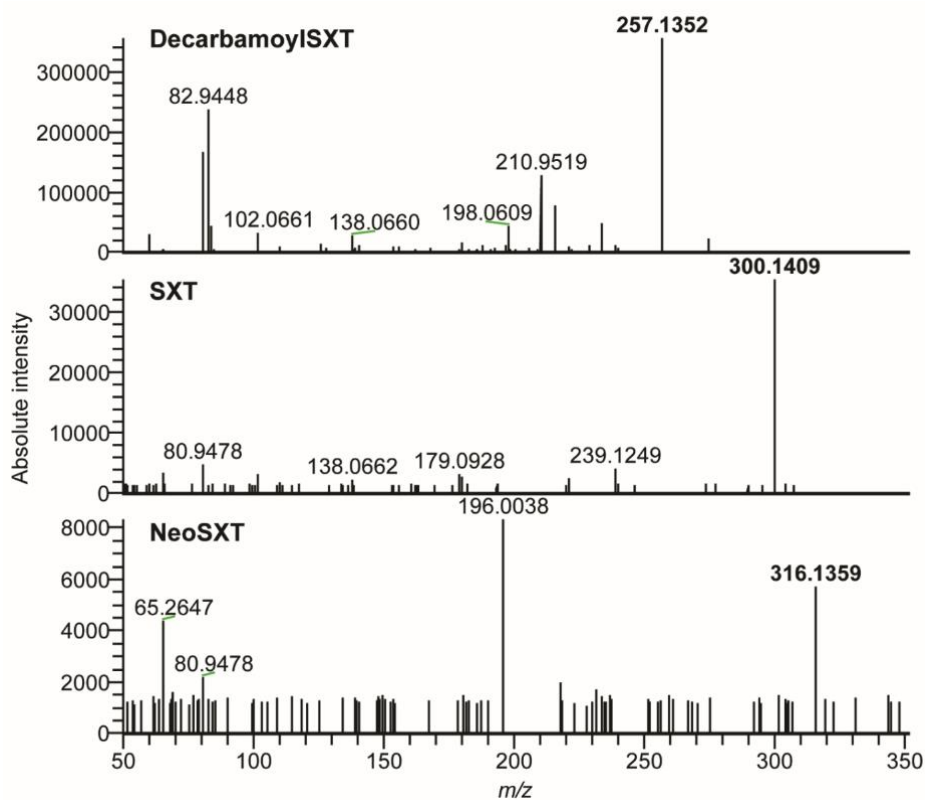


Figure 19 PSP toxins detection with UHPLC-HR-MS/MS in cell extracts of *A. minutum* RCC3008. The 300.1409, 257.1352 and 316.1359 m/z for $[M+H]^+$ assigned to decarbamoyl saxitoxin, Saxitoxin (SXT), neosaxitoxin (neoSXT) are detected at 0.8 min, respectively.

4. Results & Discussion

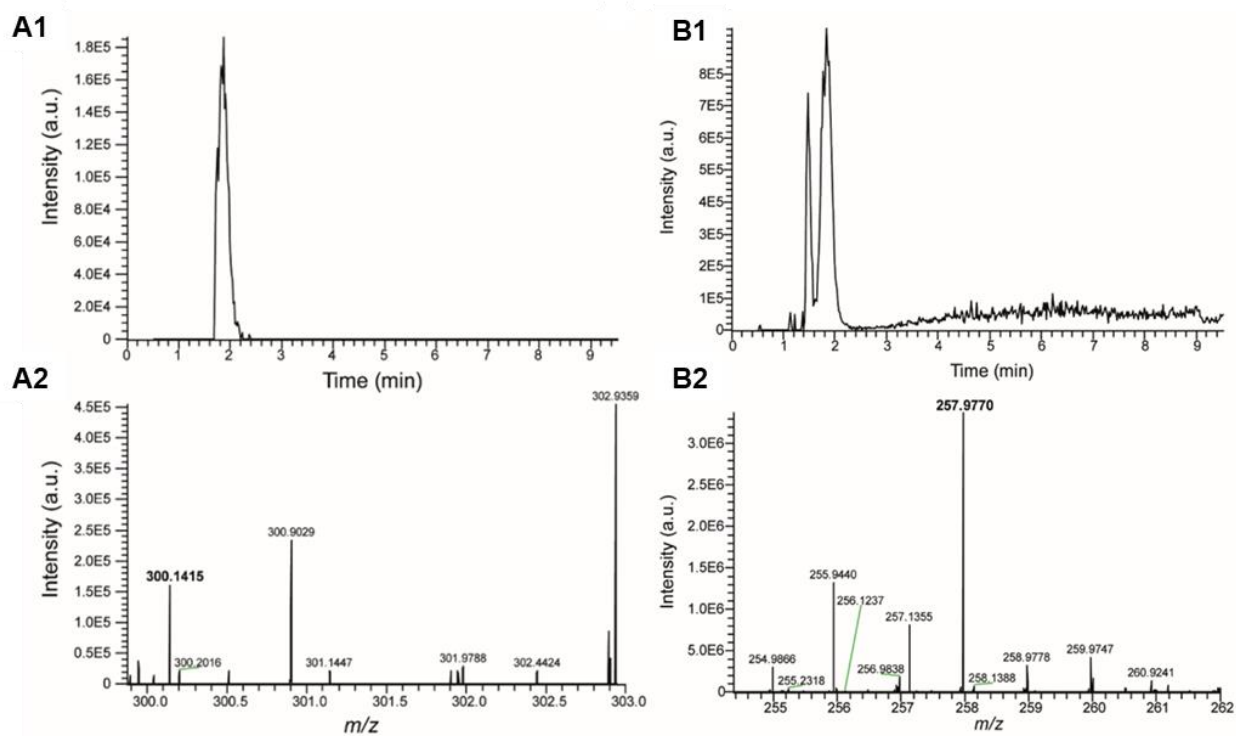


Figure 20 A) Extract ion chromatogram of *Alexandrium* cell extracts (sample E8_C19_AM176 for strain RCC3008) analyzed by UHPLC-HR-MS in positive polarity and mass spectrum with the detected m/z in bold for saxitoxin ($C_{10}H_{17}N_7O_4$ expected 300.1414 m/z for $[M+H]^+$) B) Extract ion chromatogram of *Alexandrium* cell extracts (sample E8_C19_AM176 for strain RCC3008) analyzed by UHPLC-HR-MS in positive polarity and mass spectrum with the detected m/z in bold for decarbamoylsaxitoxin ($C_9H_{16}N_6O_3$ expected 257.1356 m/z for $[M+H]^+$)

4. Results & Discussion

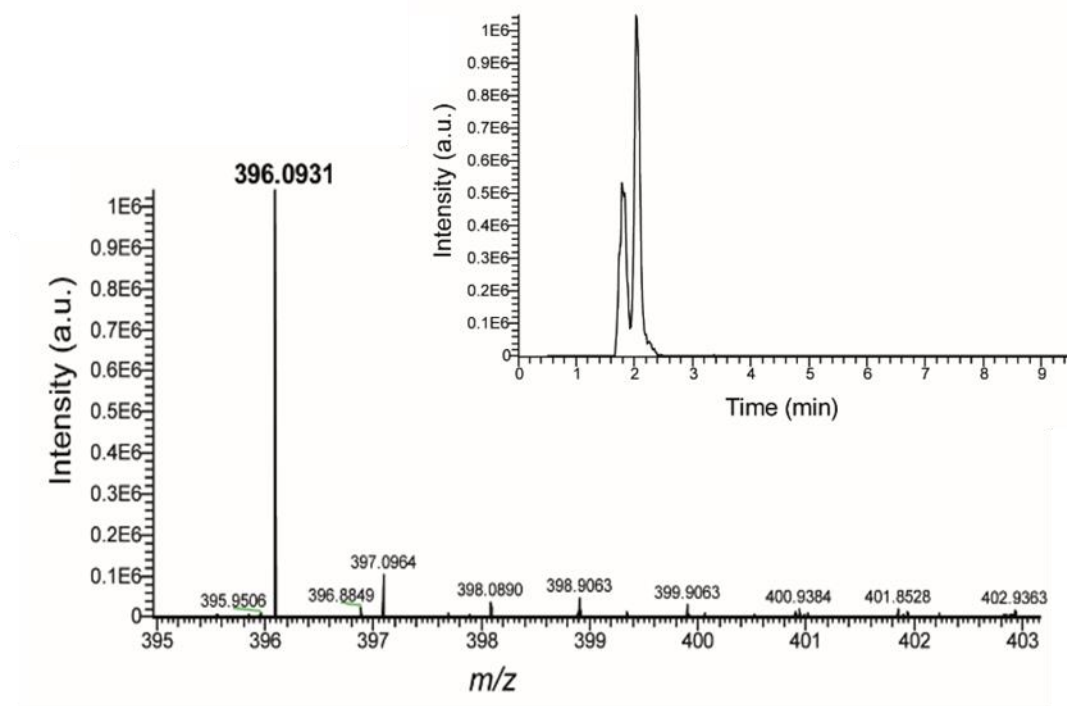


Figure 21 Extract ion chromatogram of *Alexandrium* cell extracts (sample E8_C19_AM176 for strain RCC3008) analyzed by UHPLC-HR-MS in positive polarity and mass spectrum with the detected m/z in bold for gonyautoxin 2 ($C_{10}H_{17}N_7O_8S$ expected 396.0932 m/z for $[M+H]^+$)

Generally, it can be said that PSP toxins can be detected by both columns, but those methods have to be further elaborated. The double peaks in both columns can be caused by the fact that the concentration of the sample quantity was too high, dilution would be sufficient. On the other hand, it would be better to modify the reversed-phase to the respective method to reduce the intensity of the peaks. The water content can be reduced at the beginning, also the time for the addition of acetonitrile can be reduced. It should also be mentioned that only a control solution of *A. minutum* RCC3008 from test series 4 of the synthetic copepodamides treatment was used for the detection of PSP toxins. It is therefore not possible to say whether the concentration of toxins changes in treated cells. This would be a far point to work on in the future. In order to be sure that the toxins are the one we expect, it is necessary to finally compare them with the respective standards. For a further analysis of all extracts, the samples were sent to the collaborator Erik Selander at Gothenburg University.

5. Conclusion

The main aspect of this thesis was the investigation of dinoflagellates-parasite interaction. Three main experiments were conducted to investigate the model of *Parvilucifera*-dinoflagellates interaction. To begin the study, the effect of the culture medium on the growth of *Alexandrium minutum* in healthy as well as in an infected state with *Parvilucifera rostrata* was investigated to find a medium where the infection can best spread. Concerning healthy cells, it was found that the Penzé medium is good if the highest concentration is required within the first 3 days. This is important for our work, as we aim for an incubation period of 3 days for the further course of later experiments. However, it should be noted that the growth rate for media with a higher salinity rate gives a better growth rate over a longer period of time. For this reason, it is recommended to use media with a higher salinity if the research is to continue beyond three days.

On the other hand, no statement could be made about the growth rate of the infected cells. However, this experiment proved that the infection reached its zenith between the 10th and 14th day. This could be helpful for further experiments in which the metabolites, as well as the physiology of trophocysts and sporangia, have to be determined.

For further determination of the infection, datasets of the preparation for the master thesis was used, to find out if there is a difference in the susceptibility of the different dinoflagellates *Heterocapsa triquetra* and *Alexandrium minutum* to different parasitoids. The growth rates of *H. triquetra* and *A. minutum* were evaluated independently. For *H. triquetra*, no statistically significant differences in the growth rate between healthy and infected cells could be observed, but for *A. minutum*, a decrease in the growth rate of infected cells can be observed. *H. triquetra* also has a longer incubation period until the infection is successful. This could be the first indication that *H. triquetra* has a higher immunity against *Parvilucifera* spp. A further indication for this could be the much larger number of detected and identified metabolites by UHPLC-MS/MS and CompoundDiscovererTM. In particular, a large number of different steroid- and sterol derivatives have been discovered for *H. triquetra*, which may be involved in the increased immunity.

5. Conclusion

To investigate the toxicity of individual dinoflagellates, another series of experiments was performed with a copepodamides extract and a synthetic copepodamides to stimulate toxin production. Subsequently, the samples were reinfected with *Parvilucifera rostrata*. By comparing the cell density, it could again be demonstrated that statistically significant differences between healthy and untreated cells of all *A. minutum* strains are present. Likewise, for *H. triquetra* no statistically significant difference between healthy and treated cells is possible. This indicates that treatment with copepodamides has a mainly negative effect on the cell density of toxic dinoflagellates. After infection with *P. rostrata*, no difference in growth rate can be observed, neither for *H. triquetra* nor for one of the *A. minutum* strains. This could be an indication that the induction of toxin production was successful and that *A. minutum*, therefore, developed a higher resistance to the parasitoids.

In the further analysis of the toxic dinoflagellate *A. minutum* amino acids with leucine as the terminal unit could be identified as metabolites in treated cells. This is interesting in that the dinoflagellate *Amphidinium carterae* produces 3-hydroxyacyl-CoA-dehydrogenase (HADH) during stress, which splits off leucine, valine and isoleucine units. This leads to the hypothesis that a similar reaction might occur when the cells are infected with *P. rostrata*. To verify this hypothesis, an inhibitor of HADH can be used for further experiments in order to subsequently check whether a further increased concentration of amino acids is detected.

Also, the use of ZIC-HILIC and RP synergy allowed the detection of Saxitoxin as well as derivatives of Saxitoxin in control samples. This provided confirmation that the *A. minutum* strains used were toxic dinoflagellates. The detection of steroids and sterols in *H. triquetra*, which is responsible for a possible immunity against *Parvilucifera* spp. and further analysis of the toxin production in dinoflagellates treated with copepodamides and which were infected, offer a multitude of further interesting results for the future. So, for further analysis of all extracts with the treatment with copepodamides, the samples were sent to the collaborator Erik Selander at Gothenburg University.

References

1. Field, C. B.; Behrenfeld, M. J.; Randerson, J. T.; Falkowski, P., Primary production of the biosphere: integrating terrestrial and oceanic components. *Science* **1998**, *281* (5374), 237-40.
2. Falkowski, P. G. *et al.*, The evolution of modern eukaryotic phytoplankton. *Science* **2004**, *305* (5682), 354-60.
3. Worden, A. Z. *et al.*, Environmental science. Rethinking the marine carbon cycle: factoring in the multifarious lifestyles of microbes. *Science* **2015**, *347* (6223), 1257594.
4. Siegel, D. A.; Franz, B. A., Oceanography: Century of phytoplankton change. *Nature* **2010**, *466* (7306), 569, 571.
5. Ernesto Fattorusso, W. H. G., Orazio Tagliatela-Scafati, *Handbook of Marine Natural Products*. Springer Science, Business Media B.V: 2012.
6. Ismael, A. A., Succession of heterotrophic and mixotrophic dinoflagellates as well as autotrophic microplankton in the harbour of Alexandria, Egypt. *J Plankton Res* **2003**, *25* (2), 193-202.
7. Mohamed, Z. A.; Al-Shehri, A. M., Occurrence and germination of dinoflagellate cysts in surface sediments from the Red Sea off the coasts of Saudi Arabia. *Oceanologia* **2011**, *53* (1), 121-136.
8. Hoppenrath, M.; Leander, B. S., Dinoflagellate Phylogeny as Inferred from Heat Shock Protein 90 and Ribosomal Gene Sequences. *Plos One* **2010**, *5* (10).
9. Okamoto, N.; Horak, A.; Keeling, P. J., Description of two species of early branching dinoflagellates, *Psammosa pacifica* n. g., n. sp. and *P. atlantica* n. sp. *Plos One* **2012**, *7* (6), e34900.
10. Bachvaroff, T. R.; Gornik, S. G.; Concepcion, G. T.; Waller, R. F.; Mendez, G. S.; Lippmeier, J. C.; Delwiche, C. F., Dinoflagellate phylogeny revisited: using ribosomal proteins to resolve deep branching dinoflagellate clades. *Mol Phylogenet Evol* **2014**, *70*, 314-22.
11. Jeong, H. J., The ecological roles of heterotrophic dinoflagellates in marine planktonic community. *J Eukaryot Microbiol* **1999**, *46* (4), 390-396.

References

12. Lee, H. *et al.*, Prey-dependent retention of dimethylsulfoniopropionate (DMSP) by mixotrophic dinoflagellates. *Environ Microbiol* **2012**, *14* (3), 605-616.
13. Yoo, Y. D. *et al.*, Feeding by Phototrophic Red-Tide Dinoflagellates on the Ubiquitous Marine Diatom *Skeletonema costatum*. *J Eukaryot Microbiol* **2009**, *56* (5), 413-420.
14. Miller, J. J.; Delwiche, C. F.; Coats, D. W., Ultrastructure of *Amoebophrya* sp and its Changes during the Course of Infection. *Protist* **2012**, *163* (5), 720-745.
15. Coffroth, M. A.; Santos, S. R., Genetic diversity of symbiotic dinoflagellates in the genus *Symbiodinium*. *Protist* **2005**, *156* (1), 19-34.
16. Prince, E. K.; Myers, T. L.; Naar, J.; Kubanek, J., Competing phytoplankton undermines allelopathy of a bloom-forming dinoflagellate. *Proc Biol Sci* **2008**, *275* (1652), 2733-41.
17. Alacid, E.; Rene, A.; Garces, E., New Insights into the Parasitoid *Parvilucifera sinerae* Life Cycle: The Development and Kinetics of Infection of a Bloom-forming Dinoflagellate Host. *Protist* **2015**, *166* (6), 677-699.
18. Chang, F. H.; Anderson, D. M.; Kulis, D. M.; Till, D. G., Toxin production of *Alexandrium minutum* (Dinophyceae) from the Bay of Plenty, New Zealand. *Toxicon* **1997**, *35* (3), 393-409.
19. Wiese, M. *et al.*, Neurotoxic alkaloids: saxitoxin and its analogs. *Mar Drugs* **2010**, *8* (7), 2185-211.
20. Hernandez-Becerril, D. U. *et al.*, Toxic and harmful marine phytoplankton and microalgae (HABs) in Mexican Coasts. *J Environ Sci Health A Tox Hazard Subst Environ Eng* **2007**, *42* (10), 1349-63.
21. Anderson, D. M., Toxic Red Tides and Harmful Algal Blooms - a Practical Challenge in Coastal Oceanography. *Rev Geophys* **1995**, *33*, 1189-1200.
22. Hansen, G.; Daugbjerg, N.; Franco, J. M., Morphology, toxin composition and LSU rDNA phylogeny of *Alexandrium minutum* (Dinophyceae) from Denmark, with some morphological observations on other European strains. *Harmful Algae* **2003**, *2* (4), 317-335.
23. Lewis, A. M. *et al.*, A review of the global distribution of *Alexandrium minutum* (Dinophyceae) and comments on ecology and associated paralytic shellfish toxin profiles, with a focus on Northern Europe. *J Phycol* **2018**, *54* (5), 581-598.

References

24. Touzet, N., Influence of inorganic nutrition on growth and PSP toxin production of *Alexandrium minutum* (Dinophyceae) from Cork Harbour, Ireland. **2007**.
25. Touzet, N.; Franco, J. M.; Raine, R., Characterization of nontoxic and toxin-producing strains of *Alexandrium minutum* (Dinophyceae) in Irish coastal waters. *Appl Environ Microbiol* **2007**, *73* (10), 3333-3342.
26. L. B. *et al.*, Harmful algal blooms and shellfish aquaculture in changing environment. *Bulletin of Japan Fisheries Research and Education Agency* **2019**, *49*, 73-79.
27. Landsberg, J. H., The effects of harmful algal blooms on aquatic organisms. *Rev Fish Sci* **2002**, *10* (2), 113-390.
28. Fabioux, C. *et al.*, Exposure to toxic *Alexandrium minutum* activates the detoxifying and antioxidant systems in gills of the oyster *Crassostrea gigas*. *Harmful Algae* **2015**, *48*, 55-62.
29. Pretty, J. N. *et al.*, Environmental costs of freshwater eutrophication in England and Wales. *Environ Sci Technol* **2003**, *37* (2), 201-208.
30. Sanseverino, I. *et al.*, Algal bloom and its economic impact. service, T. E. C. s. s. a. k., Ed. Publications Office of the European Union, 2016.
31. Kouakou, C. R. C.; Poder, T. G., Economic impact of harmful algal blooms on human health: a systematic review. *J Water Health* **2019**, *17* (4), 499-516.
32. Patricio A. Díaz, *et al.*, Impacts of harmful algal blooms on the aquaculture industry: Chile as a case study. *Perspectives in Phycology* **2019**, *6* (1-2), 39-50.
33. de Magalhaes, V. F.; Soares, R. M.; Azevedo, S. M. F. O., Microcystin contamination in fish from the Jacarepagua Lagoon (Rio de Janeiro, Brazil): ecological implication and human health risk. *Toxicon* **2001**, *39* (7), 1077-1085.
34. Lee, S. *et al.*, Fresh produce and their soils accumulate cyanotoxins from irrigation water: Implications for public health and food security. *Food Res Int* **2017**, *102*, 234-245.
35. Anderson, D. M., Approaches to monitoring, control and management of harmful algal blooms (HABs). *Ocean & Coastal Management* **2009**, *52* (7), 342-347.
36. Chambouvet, A.; Morin, P.; Marie, D.; Guillou, L., Control of toxic marine dinoflagellate blooms by serial parasitic killers. *Science* **2008**, *322* (5905), 1254-7.
37. Ho, J. C.; Michalak, A. M., Challenges in tracking harmful algal blooms: A synthesis of evidence from Lake Erie. *Journal of Great Lakes Research* **2015**, *41* (2), 317-325.

References

38. Kremp, A., Diversity of dinoflagellate life cycles: facets and implications of complex strategies. *Micropaleaeontologic* **2013**, 197-205.
39. Bravo, I.; Figueroa, R. I., Towards an Ecological Understanding of Dinoflagellate Cyst Functions. *Microorganisms* **2014**, 2 (1), 11-32.
40. Anderson, D. M. *et al.*, The globally distributed genus *Alexandrium*: multifaceted roles in marine ecosystems and impacts on human health. *Harmful Algae* **2012**, 14, 10-35.
41. Flynn, K. *et al.*, Changes in Toxin Content, Biomass and Pigments of the Dinoflagellate *Alexandrium minutum* during Nitrogen Refeeding and Growth into Nitrogen or Phosphorus Stress. *Mar Ecol Prog Ser* **1994**, 111 (1-2), 99-109.
42. Anderson, D. M.; Kulis, D. M.; Sullivan, J. J.; Hall, S., Toxin composition variations in one isolate of the dinoflagellate *Alexandrium fundyense*. *Toxicon* **1990**, 28 (8), 885-93.
43. Ciminiello, P.; Fattorusso, E.; Forino, M.; Montresor, M., Saxitoxin and neosaxitoxin as toxic principles of *Alexandrium andersoni* (Dinophyceae) from the Gulf of Naples, Italy. *Toxicon* **2000**, 38 (12), 1871-1877.
44. Laabir, M. *et al.*, Influence of Environmental Factors on the Paralytic Shellfish Toxin Content and Profile of *Alexandrium catenella* (Dinophyceae) Isolated from the Mediterranean Sea. *Marine Drugs* **2013**, 11 (5), 1583-1601.
45. Mikami, K.; Takeda, T.; Shimada, H.; Kimura, M., Toxin profile of the giant scallop *Mizuhopecten* (Patinopecten) yessoensis fed on the toxic dinoflagellate *Alexandrium tamarense* in laboratory, with special reference to toxicity in body parts and toxicity change during detoxification. *Nippon Suisan Gakk* **2017**, 83 (2), 225-225.
46. Han, M.; Lee, H.; Anderson, D. M.; Kim, B., Paralytic shellfish toxin production by the dinoflagellate *Alexandrium pacificum* (Chinhae Bay, Korea) in axenic, nutrient-limited chemostat cultures and nutrient-enriched batch cultures. *Mar Pollut Bull* **2016**, 104 (1-2), 34-43.
47. Trainer, V. L.; Baden, D. G.; Catterall, W. A., Detection of marine toxins using reconstituted sodium channels. *J AOAC Int* **1995**, 78 (2), 570-3.
48. Cusick, K. D.; Saylor, G. S., An overview on the marine neurotoxin, saxitoxin: genetics, molecular targets, methods of detection and ecological functions. *Mar Drugs* **2013**, 11 (4), 991-1018.

References

49. Catterall, W. A., Neurotoxins That Act on Voltage-Sensitive Sodium-Channels in Excitable-Membranes. *Annu Rev Pharmacol* **1980**, *20*, 15-43.
50. Catterall, W. A.; Morrow, C. S.; Hartshorne, R. P., Neurotoxin Binding to Receptor-Sites Associated with Voltage-Sensitive Sodium-Channels in Intact, Lysed, and Detergent-Solubilized Brain Membranes. *J Biol Chem* **1979**, *254* (22), 1379-1387.
51. Spektrum Akademischer Verlag, H. Natriumkanäle. <https://www.spektrum.de/lexikon/biologie/natriumkanale/45413> (01.12.2019)
52. Llewellyn, L. E., Saxitoxin, a toxic marine natural product that targets a multitude of receptors. *Nat Prod Rep* **2006**, *23* (2), 200-222.
53. Schantz, E. J. *et al.*, Paralytic Shellfish Poison .4. A Procedure for the Isolation and Purification of the Poison from Toxic Clam and Mussel Tissues. *J Am Chem Soc* **1957**, *79* (19), 5230-5235.
54. Wang, D. Z., Neurotoxins from marine dinoflagellates: A brief review. *Marine Drugs* **2008**, *6* (2), 349-371.
55. Molica, R. J. R. *et al.*, Occurrence of saxitoxins and an anatoxin-a(s)-like anticholinesterase in a Brazilian drinking water supply. *Harmful Algae* **2005**, *4* (4), 743-753.
56. Clemente, Z. *et al.*, Analyses of paralytic shellfish toxins and biomarkers in a southern Brazilian reservoir. *Toxicon* **2010**, *55* (2-3), 396-406.
57. Berry, J. P.; Lind, O., First evidence of "paralytic shellfish toxins" and cylindrospermopsin in a Mexican freshwater system, Lago Catemaco, and apparent bioaccumulation of the toxins in "tegogolo" snails (*Pomacea patula catemacensis*). *Toxicon* **2010**, *55* (5), 930-938.
58. Codd, G. A., Cyanobacterial toxins: Occurrence, properties and biological significance. *Water Sci Technol* **1995**, *32* (4), 149-156.
59. Liu, Y. M. *et al.*, First report of aphantoxins in China - waterblooms of toxigenic *Aphanizomenon flos-aquae* in Lake Dianchi. *Ecotox Environ Safe* **2006**, *65* (1), 84-92.
60. Kao, C. Y., Tetrodotoxin Saxitoxin and Their Significance in Study of Excitation Phenomena. *Pharmacol Rev* **1966**, *18* (2), 997-+.
61. Kao, C. Y.; Walker, S. E., Active groups of saxitoxin and tetrodotoxin as deduced from actions of saxitoxin analogues on frog muscle and squid axon. *J Physiol* **1982**, *323*, 619-37.

References

62. Bricelj, V. M.; Connell, L.; Konoki, K.; Macquarrie, S. P.; Scheuer, T.; Catterall, W. A.; Trainer, V. L., Sodium channel mutation leading to saxitoxin resistance in clams increases risk of PSP. *Nature* **2005**, *434* (7034), 763-7.
63. Sakamoto, S.; Sato, S.; Ogata, T.; Kodama, M., Formation of intermediate conjugates in the reductive transformation of gonyautoxins to saxitoxins by thiol compounds. *Fisheries Sci* **2000**, *66* (1), 136-141.
64. Yotsu-Yamashita, M. *et al.*, The structure of zetekitoxin AB, a saxitoxin analog from the Panamanian golden frog *Atelopus zeteki*: A potent sodium-channel blocker. *P Natl Acad Sci USA* **2004**, *101* (13), 4346-4351.
65. Shimizu, Y. *et al.*, Biosynthesis of saxitoxin analogs: the unexpected pathway. *J Am Chem Soc* **1984**, *106* (21), 6433-6434.
66. Lassus, P. *et al.*, Comparative efficiencies of different non-toxic microalgal diets in detoxification of PSP-contaminated oysters (*Crassostrea gigas* Thunberg). *J Nat Toxins* **2000**, *9* (1), 1-12.
67. Sullivan, J. J.; Iwaoka, W. T.; Liston, J., Enzymatic transformation of PSP toxins in the littleneck clam (*Protothaca staminea*). *Biochem Biophys Res Commun* **1983**, *114* (2), 465-72.
68. Shimizu, Y.; Yoshioka, M., Transformation of paralytic shellfish toxins as demonstrated in scallop homogenates. *Science* **1981**, *212* (4494), 547-9.
69. Llewellyn, L.; Negri, A.; Quilliam, M., High affinity for the rat brain sodium channel of newly discovered hydroxybenzoate saxitoxin analogues from the dinoflagellate *Gymnodinium catenatum*. *Toxicon* **2004**, *43* (1), 101-4.
70. Shimizu, Y., Chemistry and Mechanism of Action. In *Seafood and freshwater toxins, pharmacology, physiology and detection*, Botana, L. M., Ed. Marcel Dekker, Inc.: 2000; p 151.
71. Tammilehto, A. *et al.*, Induction of domoic acid production in the toxic diatom *Pseudo-nitzschia seriata* by calanoid copepods. *Aquat Toxicol* **2015**, *159*, 52-61.
72. Skovgaard, A., Dirty Tricks in the Plankton: Diversity and Role of Marine Parasitic Protists. *Acta Protozool* **2014**, *53* (1), 51-62.
73. Brussaard, C. P., Viral control of phytoplankton populations. *J Eukaryot Microbiol* **2004**, *51* (2), 125-38.

References

74. Park, M. G.; Yih, W.; Coats, D. W., Parasites and phytoplankton, with special emphasis on dinoflagellate infections. *J Eukaryot Microbiol* **2004**, *51* (2), 145-55.
75. Jeon, B. S.; Nam, S. W.; Kim, S.; Park, M. G., Revisiting the *Parvilucifera infectans* / *P. sinerae* (Alveolata, Perkinsozoa) species complex, two parasitoids of dinoflagellates. *Algae* **2018**, *33* (1), 1-19.
76. de Vargas, C. *et al.*, Eukaryotic plankton diversity in the sunlit ocean. *Science* **2015**, *348* (6237).
77. Moore, R. B. *et al.*, A photosynthetic alveolate closely related to apicomplexan parasites (vol 451, pg 959, 2008). *Nature* **2008**, *452* (7189), 900-900.
78. Mackin, J. G.; Owen, H. M.; Collier, A., Preliminary Note on the Occurrence of a New Protistan Parasite, Dermocystidium-Marinum N-Sp in Crassostrea-Virginica (Gmelin). *Science* **1950**, *111* (2883), 328-329.
79. Siddall, M. E.; Reece, K. S.; Graves, J. E.; Burreson, E. M., 'Total evidence' refutes the inclusion of Perkinsus species in the phylum Apicomplexa. *Parasitology* **1997**, *115*, 165-176.
80. Johansson, M.; Eiler, A.; Tranvik, L.; Bertilsson, S., Distribution of the dinoflagellate parasite *Parvilucifera infectans* (Perkinsozoa) along the Swedish coast. *Aquatic Microbial Ecology* **2006**, *43*, 289-302.
81. Garcés, E. *et al.*, *Parvilucifera sinerae* (Alveolata, Myzozoa) is a Generalist Parasitoid of Dinoflagellates. *Protist* **2013**, *164* (2), 245-260.
82. Garcés Pieres, *et al.*, Host-parasite interactions: The *Parvilucifera sinerae* model in marine microalgae. Universitat Politècnica de Catalunya, 2017.
83. Lepelletier, F. *et al.*, *Parvilucifera rostrata* sp. nov. (Perkinsozoa), a novel parasitoid that infects planktonic dinoflagellates. *Protist* **2014**, *165* (1), 31-49.
84. Jephcott, T. G. *et al.*, Ecological impacts of parasitic chytrids, syndiniales and perkinsids on populations of marine photosynthetic dinoflagellates. *Fungal Ecology* **2016**, *19*, 47-58.
85. Alacid, E.; Park, M. G.; Turon, M.; Petrou, K.; Garcés, E., A Game of Russian Roulette for a Generalist Dinoflagellate Parasitoid: Host Susceptibility Is the Key to Success. **2016**, *7* (769).

References

86. Raberg, L.; Alacid, E.; Garces, E.; Figueroa, R., The potential for arms race and Red Queen coevolution in a protist host-parasite system. *Ecol Evol* **2014**, *4* (24), 4775-85.
87. Reñé, A.; Alacid, E.; Ferrera, I.; Garcés, E., Evolutionary Trends of Perkinsozoa (Alveolata) Characters Based on Observations of Two New Genera of Parasitoids of dinoflagellates, *Dinovorax* gen. nov. and *Snorkelia* gen. nov. **2017**, *8* (1594).
88. Erard-Le Denn, E.; Chretiennot-Dinet, M. J.; Probert, I., First report of parasitism on the toxic dinoflagellate *Alexandrium minutum* Halim. *Estuar Coast Shelf S* **2000**, *50* (1), 109-113.
89. Noren, F.; Moestrup, O.; Rehnstam-Holm, A. S., *Parvilucifera infectans* Noren et Moestrup gen. et sp nov (Perkinsozoa phylum nov.): a parasitic flagellate capable of killing toxic microalgae. *Eur J Protistol* **1999**, *35* (3), 233-254.
90. Kohn, A. J., Ecology and classification of North American freshwater invertebrates. *Choice: Current Reviews for Academic Libraries* **2010**, *48* (1), 120-121.
91. Selander, E. *et al.*, Predator lipids induce paralytic shellfish toxins in bloom-forming algae. *Proc Natl Acad Sci U S A* **2015**, *112* (20), 6395-400.
92. Selander, E.; Thor, P.; Toth, G.; Pavia, H., Copepods induce paralytic shellfish toxin production in marine dinoflagellates. *Proc Biol Sci* **2006**, *273* (1594), 1673-80.
93. Guisande, C. *et al.*, Ecological advantages of toxin production by the dinoflagellate *Alexandrium minutum* under phosphorus limitation. *Mar Ecol Prog Ser* **2002**, *225*, 169-176.
94. Wolfe, G. V., The chemical defense ecology of marine unicellular plankton: Constraints, mechanisms, and impacts. *Biol Bull-U S* **2000**, *198* (2), 225-244.
95. Hayashi, R.; Saito, H.; Okumura, M.; Kondo, F., Cell bioassay for paralytic shellfish poisoning (PSP): comparison with postcolumn derivatization liquid chromatographic analysis and application to the monitoring of PSP in shellfish. *J Agric Food Chem* **2006**, *54* (2), 269-73.
96. Luckas, B., Phycotoxins in seafood--toxicological and chromatographic aspects. *J Chromatogr* **1992**, *624* (1-2), 439-56.
97. Bates, H. A.; Kostriken, R.; Rapoport, H., A chemical assay for saxitoxin. Improvements and modifications. *J Agric Food Chem* **1978**, *26* (1), 252-4.
98. Bates, H. A.; Rapoport, H., A chemical assay for saxitoxin, the paralytic shellfish poison. *J Agric Food Chem* **1975**, *23* (2), 237-9.

References

99. Gawley, R. E. *et al.*, Visible fluorescence chemosensor for saxitoxin. *J Org Chem* **2007**, *72* (6), 2187-2191.
100. Luckas, B., Chemical Analysis of PSP Toxins. In *Seafood and freshwater toxins, pharmacology, physiology and detection*, Botana, L. M., Ed. Marcel Dekker, Inc.: 2000; p 173.
101. Jaim, E.; Hummert, C.; Hess, P.; Luckas, B., Determination of paralytic shellfish poisoning toxins by high-performance ion-exchange chromatography. *J Chromatogr A* **2001**, *929* (1-2), 43-9.
102. Sullivan, J.; Wekell, M.; Kentala, L., Application of HPLC for the Determination of PSP Toxins in Shellfish. *Journal of Food Science* **2006**, *50*, 26-29.
103. Lawrence, J. F.; Menard, C.; Charbonneau, C. F.; Hall, S., A study of ten toxins associated with paralytic shellfish poison using prechromatographic oxidation and liquid chromatography with fluorescence detection. *J Assoc Off Anal Chem* **1991**, *74* (2), 404-9.
104. Quilliam, M. A.; Janecek, M.; Lawrence, J. F., Characterization of the oxidation products of paralytic shellfish poisoning toxins by liquid chromatography/mass spectrometry. *Rapid Commun Mass Spectrom* **1993**, *7* (6), 482-7.
105. Thibault, P.; Pleasance, S.; Laycock, M. V., Analysis of paralytic shellfish poisons by capillary electrophoresis. *Journal of Chromatography A* **1991**, *542*, 483-501.
106. Alacid, E.; Rene, A.; Camp, J.; Garces, E., In situ Occurrence, Prevalence and Dynamics of *Parvilucifera* Parasitoids during Recurrent Blooms of the Toxic Dinoflagellate *Alexandrium minutum*. *Frontiers in microbiology* **2017**, *8*, 1624.
107. Dauta, A.; Devaux, J.; Piquemal, F.; Boumnich, L., Growth-Rate of 4 Fresh-Water Algae in Relation to Light and Temperature. *Hydrobiologia* **1990**, *207*, 221-226.
108. Esther, G., *Parvilucifera sinerae* (Alveolata, Myzozoa) is a Generalist Parasitoid of Dinoflagellates. *Protist* **2013**.
109. Strom, S. L.; Morello, T. A., Comparative growth rates and yields of ciliates and heterotrophic dinoflagellates. *J Plankton Res* **1998**, *20* (3), 571-584.
110. Lim, P. T. *e. a.*, Effect of salinity on growth and toxin production of *Alexandrium minutum* isolated from a shrimp culture pond in northern Vietnam. *J Appl Phycol* **2011**, *23* (5), 857-864.

References

111. Abdennadher, M.; Zouari, A. B.; Sahnoun, W. F.; Hamza, A., Salinity as a Growth-Regulating Factor of the Toxic Dinoflagellate *Alexandrium Minutum*. *Adv Sci Technol Inn* **2018**, 1645-1647.
112. Lim, P. T.; Ogata, T., Salinity effect on growth and toxin production of four tropical *Alexandrium* species (Dinophyceae). *Toxicon* **2005**, *45* (6), 699-710.
113. Grzebyk, D. *et al.*, Effects of salinity and two coastal waters on the growth and toxin content of the dinoflagellate *Alexandrium minutum*. *J Plankton Res* **2003**, *25* (10), 1185-1199.
114. Giner, J.-L.; Wikfors, G. H., “Dinoflagellate Sterols” in marine diatoms. *Phytochemistry* **2011**, *72* (14), 1896-1901.
115. Yang, I. *et al.*, Comparative gene expression in toxic versus non-toxic strains of the marine dinoflagellate *Alexandrium minutum*. *BMC Genomics* **2010**, *11*, 248.
116. Zhang, H. J. *et al.*, Natural anti-HIV agents. Part IV. Anti-HIV constituents from *Vatica cinerea*. *J Nat Prod* **2003**, *66* (2), 263-8.
117. Lauritano, C. *et al.*, De novo transcriptome of the cosmopolitan dinoflagellate *Amphidinium carterae* to identify enzymes with biotechnological potential. *Sci Rep* **2017**, *7* (1), 11701.
118. Araceli E Rossignoli, C. M., Helena Martin and Juan Blanco, Application of Hydrophilic Interaction Liquid Chromatography Combined with Positive and Negative Ionization Mass Spectrometry for the Analysis of PSP Toxins. *Journal of Aquaculture & Marine Biology* **2015**, *2* (2), 8.
119. Mezzari, M. P.; Walters, K.; Jelinkova, M.; Shih, M. C.; Just, C. L.; Schnoor, J. L., Gene expression and microscopic analysis of Arabidopsis exposed to chloroacetanilide herbicides and explosive compounds. A phytoremediation approach. *Plant Physiol* **2005**, *138* (2), 858-69.
120. Bayer, T.; Aranda, M.; Sunagawa, S.; Yum, L. K.; Desalvo, M. K.; Lindquist, E.; Coffroth, M. A.; Voolstra, C. R.; Medina, M., Symbiodinium transcriptomes: genome insights into the dinoflagellate symbionts of reef-building corals. *Plos One* **2012**, *7* (4), e35269.
121. Tsuchiya, S. *et al.*, Biosynthetic route towards saxitoxin and shunt pathway. *Sci Rep* **2016**, *6*, 20340.

Appendix

Appendix for Chapter 4.2

Table A 1 Sequence order of the samples analyzed with UHPLC-HR-MS , cell concentration and Solvent volume added normalized on cell count. NA: no data

Sample code	Conditions	Quality	Cell Concentration	Solvent (µL)
blankMedium_1_H T	Penzé	Blank medium	NA	30,00
HT_YC_QC1	<i>H. triquetra</i>	Pooled sample		
HT_YC_E3	<i>H. triquetra</i>	Healthy cells	1,8E+05	68,66
HT_YC_E13	<i>H. triquetra</i>	Infected by <i>P. rostrata</i>	1,7E+05	62,69
blanksolvent18a	Blank solvent			
HT_YC_E6	<i>H. triquetra</i>	Infected by <i>P. infectans</i>	3,2E+05	119,40
HT_YC_E11	<i>H. triquetra</i>	Infected by <i>P. rostrata</i>	2,2E+05	82,09
HT_YC_E9	<i>H. triquetra</i>	Infected by <i>P. infectans</i>	2,3E+05	85,07
blanksolvent18	Blank solvent			
HT_YC_QC2	<i>H. triquetra</i>	Pooled sample		
HT_YC_E15	<i>H. triquetra</i>	Infected by <i>P. rostrata</i>	1,9E+05	71,64
HT_YC_E10	<i>H. triquetra</i>	Infected by <i>P. infectans</i>	3,2E+05	117,91
blanksolvent18b2	Blank solvent			
HT_YC_E1	<i>H. triquetra</i>	Healthy cells	6,0E+05	225,37
HT_YC_E4	<i>H. triquetra</i>	Healthy cells	3,4E+05	126,87
HT_YC_E12	<i>H. triquetra</i>	Infected by <i>P. rostrata</i>	2,0E+05	74,63
blanksolvent19	Blank solvent			
HT_YC_QC3	<i>H. triquetra</i>	Pooled sample		
HT_YC_E8	<i>H. triquetra</i>	Infected by <i>P. infectans</i>	3,4E+05	125,37
HT_YC_E2	<i>H. triquetra</i>	Healthy cells	1,8E+05	67,16
Blank solvent	Blank solvent			
HT_YC_E5	<i>H. triquetra</i>	Healthy cells	2,0E+05	76,12
HT_YC_E7	<i>H. triquetra</i>	Infected by <i>P. infectans</i>	3,5E+05	129,85
HT_YC_E14	<i>H. triquetra</i>	Infected by <i>P. rostrata</i>	2,0E+05	76,12
blanksolvent20	Blank solvent			
HT_YC_QC4	<i>H. triquetra</i>	Pooled sample		
HT_YC_QC5_ID_P OS	<i>H. triquetra</i>	Identification ddMS		
HT_YC_QC5_ID_N EG	<i>H. triquetra</i>	Identification ddMS		
blankMedium_2_A M	Penzé	Blank medium	NA	30,00
AM_YC_QC1	<i>A. minutum</i>	Pooled sample		
AM_YC_E28	<i>A. minutum</i>	Infected by <i>P. rostrata</i>	1,5E+05	56,72
AM_YC_E19	<i>A. minutum</i>	Healthy cells	2,3E+05	86,57

Appendix

blank-solvent2b	Blank solvent			
AM_YC_E24	<i>A. minutum</i>	Infected by <i>P. infectans</i>	1,3E+05	47,76
AM_YC_E21	<i>A. minutum</i>	Infected by <i>P. infectans</i>	6,4E+04	23,88
AM_YC_E27	<i>A. minutum</i>	Infected by <i>P. rostrata</i>	1,1E+05	41,79
blank-solvent2	Blank solvent			
AM_YC_QC2	<i>A. minutum</i>	Pooled sample		
AM_YC_E25	<i>A. minutum</i>	Infected by <i>P. infectans</i>	9,6E+04	35,82
AM_YC_E22	<i>A. minutum</i>	Infected by <i>P. infectans</i>	1,5E+05	56,72
blank-solvent3b	Blank solvent			
AM_YC_E18	<i>A. minutum</i>	Healthy cells	2,1E+05	77,61
AM_YC_E16	<i>A. minutum</i>	Healthy cells	2,7E+05	100,00
AM_YC_E26	<i>A. minutum</i>	Infected by <i>P. rostrata</i>	1,9E+05	71,64

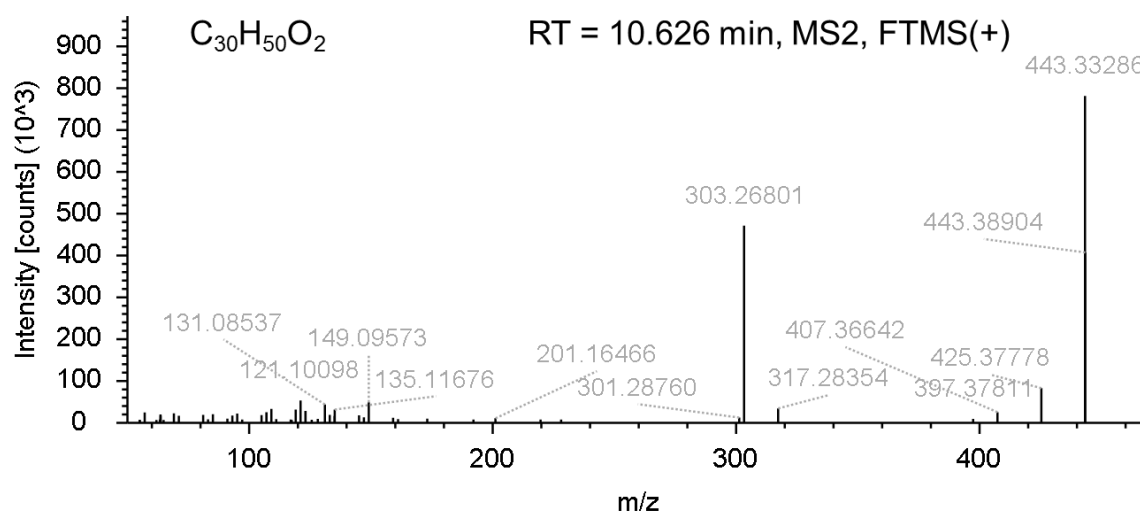


Figure A 1 MS/MS spectra obtained from the analysis with UHPLC-MS/MS of cellular extracts of *H. triquetra* in positive ion polarity obtained from precursor ion of the sterol derivate C₃₀H₅₀O₂ (Figure from CompoundDiscovererTM; RT = 10.626 min, 443.3329 *m/z* [M+H]⁺).

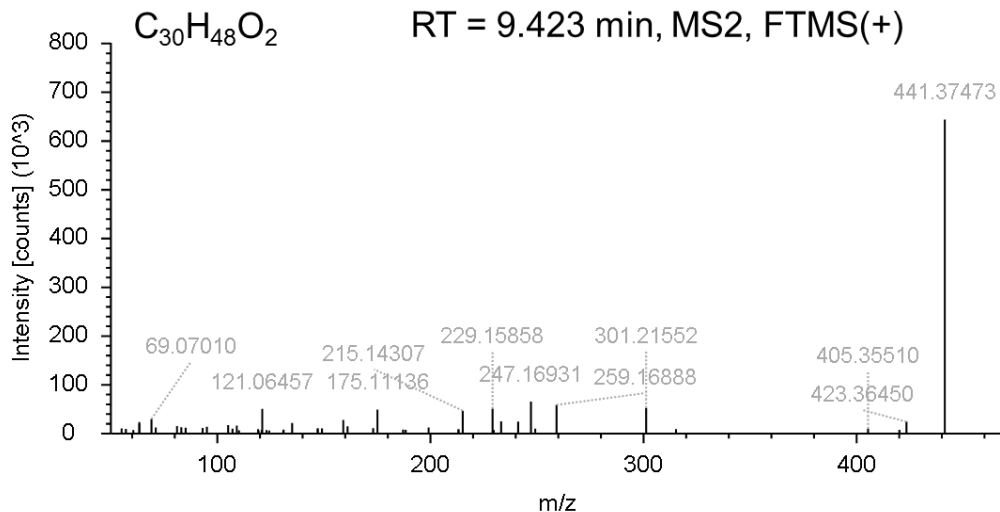


Figure A 2 MSMS spectra obtained from the analysis with UHPLC-MS/MS of cellular extracts of *H. triquetra* in positive ion polarity obtained from precursor ion of the sterol derivate C₃₀H₄₈O₂ (Figure from CompoundDiscovererTM; RT = 9.423 min, 441.3747 m/z [M+H]⁺).

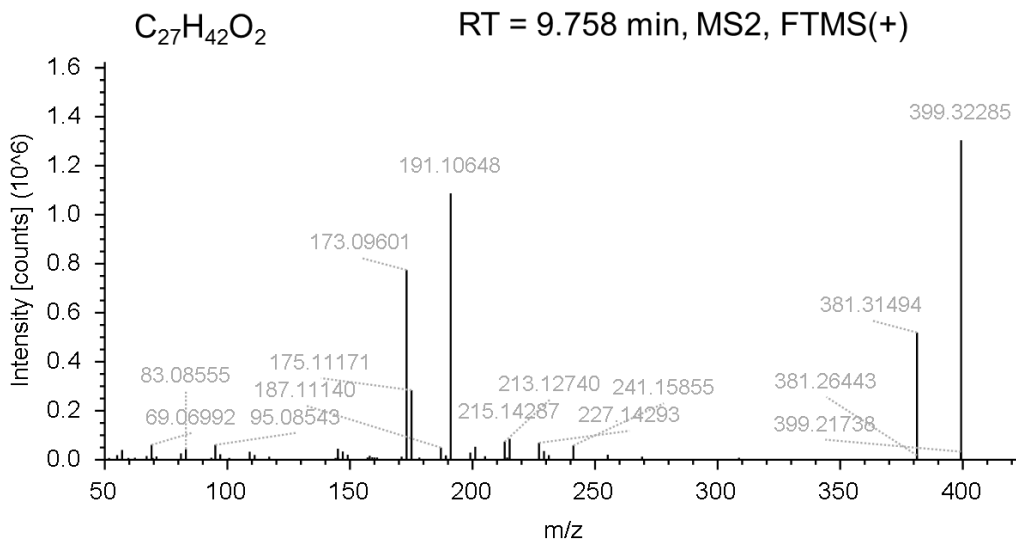


Figure A 3 MS/MS spectra obtained from the analysis with UHPLC-MS/MS of cellular extracts of *H. triquetra* in positive ion polarity obtained from precursor ion of the steroid derivate C₂₇H₄₂O₂ (Figure from CompoundDiscovererTM; RT = 9.758 min, 399.3229 m/z [M+H]⁺).

Appendix for Chapter 4.3

Table A 2 Calculated growth rate for *Alexandrium minutum* treated with the synthetic copepodamide. The difference in the mean values between the treated and untreated cultures is greater than would be expected by chance. This proves with the t-test that there is a statistically significant difference between the two treatments. (P = 0,038).

Condition	Cell count Day 0	Cell density Day 0 (cell per ml)	Cell count Day 2	Cell density Day 3 (cell per ml)	growth rate after 3 days with treatment
synthetic copepodamide 1nM	20	25000	18	22500	-0,052680258
synthetic copepodamide 1nM	20	25000	23	28750	0,069880971
synthetic copepodamide 1nM	20	25000	14	17500	-0,178337472
control - Treated with Methanol	20	25000	26	32500	0,131182132
control - Treated with Methanol	20	25000	32	40000	0,235001815
control - Treated with Methanol	20	25000	29	36250	0,185781778

Appendix

Table A 3 Calculated growth rate for *Alexandrium minutum* treated with the synthetic copepodamide. The difference in the mean values between the treated and untreated cultures is greater than would be expected by chance. This proves with the Mann-Whitney Rank sum test that there is a statistically significant difference between the two treatments. (P = 0,015)

Condition	Cell count Day 0	Cell density Day 0 (cell per ml)	Cell count Day 2	Cell density Day 3 (cell per ml)	growth rate after 3 days with treatment
synthetic copepodamide 1nM	156	195000	78	97500	-0,34657359
synthetic copepodamide 1nM	156	195000	75	93750	-0,366183947
synthetic copepodamide 1nM	156	195000	77	96250	-0,353025293
control - Treated with Methanol	156	195000	79	98750	-0,340204077
control - Treated with Methanol	156	195000	78	97500	-0,34657359
control - Treated with Methanol	156	195000	78	97500	-0,34657359
synthetic copepodamide 1nM	156	195000	45	56250	-0,621596759
synthetic copepodamide 1nM	156	195000	77	96250	-0,353025293
synthetic copepodamide 1nM	156	195000	78	97500	-0,34657359
control - Treated with Methanol	156	195000	79	98750	-0,340204077
control - Treated with Methanol	156	195000	80	100000	-0,333914686
control - Treated with Methanol	156	195000	78	97500	-0,34657359

Appendix

Table A 4 Calculated growth rate for *Alexandrium minutum* treated with the natural copepodamide. The difference in the mean values between the treated and untreated cultures is greater than would be expected by chance. This proves with the t-test that there is a statistically significant difference between the two treatments. (P = 0,010).

Condition	Cell count Day 0	Cell density Day 0 (cell per ml)	Cell count Day 2	Cell density Day 3 (cell per ml)	growth rate after 3 days with treatment
Extracts mixture copepodamides	53	66250	60	75000	0,062026324
Extracts mixture copepodamides	53	66250	61	76250	0,070290975
Extracts mixture copepodamides	53	66250	58	72500	0,045075548
control - Treated with Methanol	53	66250	65	81250	0,102047678
control - Treated with Methanol	53	66250	67	83750	0,117200353
control - Treated with Methanol	53	66250	70	87500	0,139101664

Table A 5 Calculated growth rate for *Alexandrium minutum* treated with the synthetic copepodamide. The difference in the mean values between the treated and untreated cultures is greater than would be expected by chance. This proves with the t-test that there is a statistically significant difference between the two treatments. (P = 0,030).

Condition	Cell count Day 0	Cell density Day 0 (cell per ml)	Cell count Day 2	Cell density Day 3 (cell per ml)	growth rate after 3 days with treatment
control - Treated with Methanol	71	88750	105	131250	0,195640237
control - Treated with Methanol	71	88750	116	145000	0,245455157
control - Treated with Methanol	71	88750	100	125000	0,171245154
control - Treated with Methanol	71	88750	94	117500	0,140307453
control - Treated with Methanol	71	88750	109	136250	0,214334003
synthetic copepodamide 1nM	71	88750	97	121250	0,156015551
synthetic copepodamide 1nM	71	88750	86	107500	0,09583371
synthetic copepodamide 1nM	71	88750	97	121250	0,156015551
synthetic copepodamide 1nM	71	88750	93	116250	0,134959808
synthetic copepodamide 1nM	71	88750	95	118750	0,145598507

Appendix

Table A 6 Calculated growth rate for *Alexandrium minutum* treated with the natural copepodamide. The difference in the mean values between the treated and untreated cultures is greater than would be expected by chance. This proves with the t-test that there is a statistically significant difference between the two treatments. (P = 0,024).

Condition	Cell count Day 0	Cell density Day 0 (cell per ml)	Cell count Day 2	Cell density Day 3 (cell per ml)	growth rate after 3 days with treatment
Extracts mixture copepodamides	75	93750	38	47500	-0,339950977
Extracts mixture copepodamides	75	93750	39	48750	-0,326963234
Extracts mixture copepodamides	75	93750	42	52500	-0,289909248
control - Treated with Methanol	75	93750	98	122500	0,133739683
control - Treated with Methanol	75	93750	130	162500	0,275023168
control - Treated with Methanol	75	93750	113	141250	0,204949853
Extracts mixture copepodamides	91	113750	27	33750	-0,60751132
Extracts mixture copepodamides	91	113750	21	26250	-0,733168534
Extracts mixture copepodamides	91	113750	25	31250	-0,645991841
control - Treated with Methanol	91	113750	33	41250	-0,507175973
control - Treated with Methanol	91	113750	51	63750	-0,289516937
control - Treated with Methanol	91	113750	50	62500	-0,299418251

Appendix

Table A 7 Calculated growth rate for *Alexandrium minutum* (strains AM176, RCC2672, RCC 1490, RCC2663) and *Heterocapsa triquetra* (strain HT150) treated with the synthetic copepodamide. All strains of *Alexandrium minutum* could have statistically significant differences observed. (AM176, $p = 0,004$; RCC2672, $p = 0,003$; RCC1490, $p = 0,030$; RCC2663, $p = 0,029$)

Algae strain	Cell count Day 0	Cell density Day 0 (cell per ml)	Cell count Day 2	Cell density Day 3 (cell per ml)	growth rate after 3 days with treatment
HT150	4	5000	2	2500	-0,34657359
HT150	4	5000	1	1250	-0,693147181
HT150	4	5000	13	16250	0,589327498
HT150	4	5000	16	20000	0,693147181
HT150	4	5000	10	12500	0,458145366
HT150	4	5000	9	11250	0,405465108
HT150	4	5000	10	12500	0,458145366
HT150	4	5000	22	27500	0,852374046
RCC2663	5	6250	3	3750	-0,255412812
RCC2663	5	6250	1	1250	-0,804718956
RCC2663	5	6250	1	1250	-0,804718956
RCC2663	5	6250	1	1250	-0,804718956
RCC2663	5	6250	6	7500	0,091160778
RCC2663	5	6250	5	6250	0
RCC2663	5	6250	5	6250	0
RCC2663	5	6250	7	8750	0,168236118
RCC1490	7	8750	4	5000	-0,279807894
RCC1490	7	8750	6	7500	-0,07707534
RCC1490	7	8750	5	6250	-0,168236118

Appendix

RCC1490	7	8750	4	5000	-0,279807894
RCC1490	7	8750	5	6250	-0,168236118
RCC1490	7	8750	9	11250	0,125657214
RCC1490	7	8750	8	10000	0,066765696
RCC1490	7	8750	9	11250	0,125657214
RCC2672	8	10000	6	7500	-0,143841036
RCC2672	8	10000	5	6250	-0,235001815
RCC2672	8	10000	6	7500	-0,143841036
RCC2672	8	10000	6	7500	-0,143841036
RCC2672	8	10000	9	11250	0,058891518
RCC2672	8	10000	8	10000	0
RCC2672	8	10000	8	10000	0
RCC2672	8	10000	7	8750	-0,066765696
AM176	8	10000	6	7500	-0,143841036
AM176	8	10000	5	6250	-0,235001815
AM176	8	10000	5	6250	-0,235001815
AM176	8	10000	5	6250	-0,235001815
AM176	8	10000	7	8750	-0,066765696
AM176	8	10000	8	10000	0
AM176	8	10000	9	11250	0,058891518
AM176	8	10000	9	11250	0,058891518

Zusammenfassung

Der Schwerpunkt dieser Arbeit lag bei der Untersuchung der Wechselwirkungen zwischen Dinoflagellaten und Parasiten. Drei Hauptexperimente wurden hierzu durchgeführt, um das Modell der *Parvilucifera*-Dinoflagellates Wechselwirkung zu untersuchen. Zu Beginn der Thesis wurde die Wirkung verschiedener Kulturmediums auf das Wachstum von *Alexandrium minutum*, sowohl im gesunden als auch im infizierten Zustand mit *Parvilucifera rostrata* untersucht, um ein Medium zu finden, in dem sich die Infektion am besten ausbreiten kann. Im Hinblick auf gesunde Zellen wurde festgestellt, dass das Penzé-Medium sich gut eignet, wenn innerhalb der ersten 3 Tage eine erhöhte Konzentration erwünscht ist. Dies ist wichtig für unsere Arbeit, da wir für den weiteren Verlauf späterer Experimente eine Inkubationszeit von 3 Tagen anstreben. Es ist jedoch zu beachten, dass sich für Medien mit einem höheren Salzgehalt eine höhere Wachstumsrate über einen längeren Zeitraum einspielt. Aus diesem Grund wird empfohlen, Medien mit einem höheren Salzgehalt zu verwenden, wenn die Forschung über einen längeren Zeitraum von drei Tagen hinaus geht.

Andererseits konnte keine Aussage über die Wachstumsrate der infizierten Zellen getroffen werden. In diesem Experiment wurde jedoch nachgewiesen, dass die Infektion zwischen dem 10. und 14. Tag ihren Höhepunkt erreichte. Dies könnte für weitere Experimente hilfreich sein, in denen die Metaboliten sowie die Physiologie der Trophozysten und Sporangien bestimmt werden müssen.

Für die weitere Bestimmung der Infektion wurden Datensätze der Vorbereitungszeit für die Masterarbeit verwendet, um herauszufinden, ob es einen Unterschied in der Anfälligkeit der verschiedenen Dinoflagellaten *Heterocapsa triquetra* und *Alexandrium minutum* für verschiedene Parasitoide gibt. Die Wachstumsraten von *H. triquetra* und *A. minutum* wurden unabhängig voneinander bewertet. Für *H. triquetra* konnten keine statistisch signifikanten Unterschiede in der Wachstumsrate zwischen gesunden und infizierten Zellen beobachtet werden, während für *A. minutum* ein Rückgang der Wachstumsrate infizierter Zellen beobachtet werden kann. *H. triquetra* besitzt auch eine längere Inkubationszeit, bis die Infektion erfolgreich ist. Dies könnte der erste Hinweis darauf sein, dass *H. triquetra* eine höhere Immunität gegen *Parvilucifera* spp hat, ein weiterer Hinweis dafür könnte die viel größere Anzahl der nachgewiesenen und identifizierten Metaboliten durch UHPLC-MS/MS

Zusammenfassung

und CompoundDiscoverer™ sein. So wurde insbesondere für *H. triquetra* eine Vielzahl von verschiedenen Steroid- und Sterolderivaten entdeckt, die an der erhöhten Immunität beteiligt sein könnten.

Um die Toxizität einzelner Dinoflagellate zu untersuchen, wurde eine weitere Reihe von Experimenten mit einem Copepodamid-Extrakt und einem synthetischen Copepodamid durchgeführt, die die Produktion von Giftstoffen stimulieren sollen. Anschließend wurden die Proben mit *Parvilucifera rostrata* erneut infiziert. Durch den Vergleich der Zelldichte konnte erneut nachgewiesen werden, dass statistisch signifikante Unterschiede zwischen gesunden und unbehandelten Zellen aller *A. minutum* Stämme vorliegen. Außerdem ist für *H. triquetra* kein statistisch signifikanter Unterschied zwischen gesunden und behandelten Zellen möglich. Dies deutet darauf hin, dass die Behandlung mit Copepodamiden einen hauptsächlich negativen Einfluss auf die Zelldichte von toxischen Dinoflagellaten hat. Nach der Infektion mit *P. rostrata* ist kein Unterschied in der Wachstumsrate zu beobachten, weder für *H. triquetra* noch für einen der *A. minutum* Stämme. Dies könnte ein Hinweis darauf sein, dass die Induktion der Toxinproduktion erfolgreich war und das *A. minutum* daher eine höhere Resistenz gegenüber dem Parasitoid entwickelte.

In der weiteren Analyse des toxischen Dinoflagellats *A. minutum* konnten Aminosäuren mit Leucin am C- oder N-Terminus als Metaboliten in behandelten Zellen identifiziert werden. Interessant ist, dass die Dinoflagellate *Amphidinium carterae* unter Stress 3-Hydroxyacyl-CoA-Dehydrogenase (HADH) produziert, die Leucin-, Valin- und Isoleucineinheiten abspaltet. Dieses lässt die Annahme zu, dass eine ähnliche Reaktion bei der Infizierung der Zellen mit *P. rostrata* stattfindet. Um diese Hypothese zu verifizieren, kann ein Inhibitor von HADH für weitere Experimente verwendet werden, um anschließend zu überprüfen, ob eine weiter erhöhte Konzentration dieser Aminosäuren nachweisbar ist.

Die Verwendung von ZIC-HILIC- und RP-Synergie ermöglichte den Nachweis von Saxitoxin sowie von Saxitoxinderivaten in Kontrollproben. Dies bestätigte, dass es sich bei den verwendeten *A. minutum*-Stämmen um toxische Dinoflagellaten handelte. Der Nachweis von Steroiden und Sterolen in *H. triquetra*, die für eine mögliche Immunität gegen *Parvilucifera* spp. verantwortlich sind, und die weitere Analyse der Toxinproduktion in mit Copepodamiden behandelten und infizierten Dinoflagellaten bieten eine Vielzahl weiterer

Zusammenfassung

interessanter Ergebnisse für die Zukunft. Zur weiteren Analyse aller Extrakte, die mit Copepodamiden behandelt wurden, wurden die Proben an den Kollaborateur Erik Selander von der Universität Göteborg geschickt.

Declaration of Authorship

I hereby declare that I have written this Masterthesis independently and that I have not used any sources other than those mentioned.

Selbständigkeitserklärung

Ich versichere hiermit, dass ich die vorliegende Masterarbeit selbständig verfasst und keine als die angegebenen Hilfsmittel und Quellen benutzt habe.

Ort, Datum

Unterschrift